

A FEAST SVDSOLVER FOR THE COMPUTATION OF SINGULAR VALUE DECOMPOSITIONS OF LARGE MATRICES BASED ON THE CHEBYSHEV–JACKSON SERIES EXPANSION

ZHONGXIAO JIA AND KAILIANG ZHANG

ABSTRACT. The FEAST eigensolver is extended to the computation of the singular triplets of a large matrix A with the singular values in a given interval. It is subspace iteration in nature applied to an approximate spectral projector associated with the cross-product matrix $A^T A$ and constructs approximate left and right singular subspaces corresponding to the desired singular values, onto which A is projected to obtain approximations to the desired singular triplets. Approximate spectral projectors are constructed using the Chebyshev–Jackson series expansion other than contour integration and quadrature rules, and they are proven to be always symmetric positive semi-definite with the eigenvalues in $[0, 1]$. Compact estimates are established for pointwise approximation errors of a specific step function that corresponds to the exact spectral projector, the accuracy of the approximate spectral projector, the number of desired singular triplets, the distance between the desired right singular subspace and the subspace generated each iteration, and the convergence of the FEAST SVDSolver. Practical selection strategies are proposed for the series degree and the subspace dimension. Numerical experiments illustrate that the FEAST SVDSolver is robust and efficient.

1. INTRODUCTION

Matrix singular value decomposition (SVD) problems play a crucial role in many applications. For small to moderate problems, very efficient and robust SVD algorithms and softwares have been well developed and widely used [8, 30]. They are often called direct SVD solvers and compute the entire singular values and/or singular vectors using predictable iterations. In this paper, we consider the following partial SVD problem: Given a matrix $A \in \mathbb{R}^{m \times n}$ with $m \geq n \gg 1$ and a real interval $[a, b]$ contained in the singular spectrum of A , determine the n_{sv} singular triplets (σ, u, v) with the singular values $\sigma \in [a, b]$ counting multiplicities, where

$$\begin{cases} Av = \sigma u, \\ A^T u = \sigma v, \\ \|u\| = \|v\| = 1. \end{cases}$$

2020 *Mathematics Subject Classification.* Primary 65F15, 15A18, 65F50.

Key words and phrases. singular value decomposition, Chebyshev–Jackson series, spectral projector, Jackson damping factor, pointwise convergence, subspace iteration, SVDSolver, convergence rate.

Supported in part by the National Natural Science Foundation of China (Nos. 11771249 and 12171273).

Over the past nearly two decades, a new class of numerical methods has emerged for computing the eigenvalues of a large matrix in a given region and/or the associated eigenvectors, and they are based on contour integration and rational filtering. Among them, representatives are the Sakurai–Sugiura (SS) method [28] and the FEAST eigensolver [22], which fall into the category of Rayleigh–Ritz projection methods. The SS method and subsequent variants [12–15, 29] have resulted in the z-Pares package [6] that handles the large Hermitian and non-Hermitian matrix eigenvalue problems. The original SS method is the SS-Hankel method, and its variants include the SS-RR (Rayleigh–Ritz projection) method and SS-Arnoldi method as well as their block variants. The SS-Hankel method computes certain moments constructed by the contour integral with an integral domain containing all the desired eigenvalues to form small Hankel matrices or matrix pairs and may be numerically unstable. In computations, the contour integral is approximated by a numerical quadrature, and the moments are computed approximately. The SS method and its variants are essentially Krylov or block Krylov subspace based methods, realize the Rayleigh–Ritz projection onto them, and compute Ritz approximations [15]. The SS-RR method computes an orthonormal basis of the underlying subspace and projects the large matrix or matrix pair onto it, and the SS-Arnoldi method exploits the Arnoldi process to generate an orthonormal basis of the subspace and forms the projection matrix. We refer the reader to [15] for a summary of these methods.

The FEAST eigensolver [9, 19, 22, 31], first introduced by Polizzi [22] in 2009, has led to the development of the FEAST numerical library [23]. Unlike the SS method and its variants, this eigensolver works on subspaces of a fixed dimension and uses subspace iteration [8, 21, 27, 30] to generate a sequence of subspaces, onto which the Rayleigh–Ritz projection of the original matrix or matrix pair is realized and the Ritz approximations are computed.

The SS method and the FEAST eigensolver are common in that they both use the contour integral and a numerical quadrature to construct a good approximate spectral projector associated with all the eigenvalues in the region of interest. This involves solutions of certain linear systems with shifted coefficient matrices, where the shifts are the nodes of the numerical quadrature used. Particularly, for the FEAST eigensolver, at each iteration one needs to solve several, i.e., the subspace dimension times the number of nodes, large linear systems. These linear systems are typically indefinite, and are ill conditioned whenever a node is close to some eigenvalue, so that Krylov subspace iterative methods, e.g., the GMRES or MINRES method [26], may be inefficient.

Another possible approach is to construct an approximate spectral projector by the Chebyshev or Chebyshev–Jackson series expansion, as done in, e.g., [5]. However, such approximation approach has received little attention, compared with rational approximations based on the contour integral and numerical quadratures, and it is also secondary and a by-product in [5]. Among others, a fundamental reason for this situation that accuracy estimates lacks for the Chebyshev–Jackson series and approximate spectral projector.

It is well known from, e.g., [20] that the Chebyshev series expansion is the best squares approximation to a given function with respect to the Chebyshev l_2 -norm. The function in our concern is a specific step function $h(x)$, and the researchers in [5] derive a quantitative error estimate for the Chebyshev series approximation to this

specific function in the Chebyshev l_2 -norm. Qualitatively, it is well known that the pointwise convergence of the Chebyshev series to $h(x)$ holds. Specially, the series at a discontinuity or jump point x converges to the mean $(h(x+0) + h(x-0))/2$, where $h(x+0)$ (resp. $h(x-0)$) means the limit of $h(t)$ from the right (resp. left). However, just like the rational approximation to the step function, it is the *pointwise quantitative* error of the series that matters and is critically needed. Unfortunately, such error estimates cannot be obtained from the ones with respect to the Chebyshev l_2 -norm. Remarkably, for the step function $h(x)$, it is shown in, e.g., [5] that Jackson coefficients [24] can considerably dampen Gibbs oscillations and it is better to exploit the resulting Chebyshev–Jackson series. However, just as the Chebyshev series, pointwise quantitative error estimates lack for this series. As a consequence, there is no result on the convergence of the FEAST eigensolver when using the Chebyshev–Jackson series to construct an approximate spectral projector, and nothing is known on the convergence rate of each desired eigenvalue, a reliable determination of subspace dimension and a proper selection of series degree.

Since the SVD of A is mathematically equivalent to the eigendecomposition of its cross-product matrix $A^T A$, in principle, the afore-mentioned approaches can be adapted to the computation of the singular triplets of A associated with the singular values σ in a given interval $[a, b]$. In this paper, for such a partial SVD problem, we will focus on constructing an approximate spectral projector associated with $\sigma \in [a, b]$ by exploiting the Chebyshev–Jackson series expansion. We apply subspace iteration to the approximate spectral projector constructed and, using a certain reasonable approach, generate a sequence of approximate *left* and *right* singular spaces corresponding to $\sigma \in [a, b]$. However, instead of explicitly dealing with the eigenvalue problem of $A^T A$, we work on A directly and project A onto the left and right subspaces generated and compute the Ritz approximations to the desired singular triplets. We call the resulting algorithm a FEAST SVDSolver.

We will make a detailed analysis on the pointwise convergence of the Chebyshev–Jackson series and establish quantitative *pointwise* error estimates for the series. We make full use of these results to estimate the accuracy of the approximate spectral projector, the distance between the desired right singular subspace and the approximate right singular subspace generated, and the convergence rate of each Ritz approximation computed by our FEAST SVDSolver. In the meantime, we show how to exploit randomized trace estimation results to reliably estimate the number n_{sv} of desired singular triplets with $\sigma \in [a, b]$. With this result, we are able to propose practical and robust selection strategies for the subspace dimension p and series degree.

Precisely, we prove that the value of the Chebyshev–Jackson series always lies in $[0, 1]$. By this property, we are able to prove that the approximate spectral projectors constructed are unconditionally symmetric positive semi-definite (SPSD) and their eigenvalues always lie in $[0, 1]$. This is a unique property that the approximate spectral projectors constructed by some commonly used numerical quadratures, such as the Gauss–Legendre quadrature rule and Zolotarev quadrature rule, may not possess even when they are very good approximations to the spectral projector, as is clearly seen from, e.g., [9]. An exception is the trapezoid quadrature rule, which generates an SPSD approximate spectral projector for real symmetric eigenvalue problems when all the shifted linear systems are solved accurately [9]. Since 1989 (cf. the Hutchinson’s paper [10]), several algorithms have been proposed

to reliably estimate the trace of a matrix by Monte Carlo methods [2, 11, 32]. As it turns out, the positive semi-definiteness is important and attractive since it enables us to the Rademacher random estimations in [1, 3, 25] to reliably predict the number n_{sv} of desired singular triplets and propose a practical selection strategy for the subspace dimension in the FEAST SVDsolver.

Cortinovis and Kressner [3] have derived randomized trace estimates for a symmetric indefinite matrix with Rademacher or Gaussian random vectors. Contrary to the SPSD case, their bound is for *absolute* rather than *relative* errors of the trace, and the number of samples can be much larger than that in the SPSD case; see the elaborations after Lemma 2.1 in this paper and Remark 4, Corollary 2 of [3] for Rademacher random vectors. Therefore, a reliable and efficient use of the bound in the indefinite case is far from that for the SPSD case.

All the theoretical results and algorithms in this paper are either directly applicable or trivially adaptable to the real symmetric and complex Hermitian matrix eigenvalue problems, once we replace $A^T A$ in this paper by a given symmetric matrix itself and the Rayleigh–Ritz projection for the SVD problem by that for the eigenvalue problem.

The paper is organized as follows. In section 2, we briefly review some preliminaries, the subspace iteration applied to an approximate spectral projector, and some results to be used in the paper. In section 3, we establish the quantitative pointwise convergence results on the Chebyshev–Jackson series expansion. Then we propose the FEAST SVDsolver in section 4 to compute the desired n_{sv} singular triplets of A . We establish the accuracy estimates for the approximate spectral projector and subspace dimension, and present a number of convergence results on the FEAST SVDsolver. In section 5, we count the computational cost of the FEAST SVDsolver. In section 6, we report numerical experiments to illustrate the performance of the FEAST SVDsolver, where we consider robust and practical selections of the subspace dimension p and the degree d of Chebyshev–Jackson series. Finally, we conclude the paper in section 7.

We mention that for the concerning SVD problem of a matrix $A \in \mathbb{R}^{m \times n}$ with $m < n$ we simply apply the FEAST SVDsolver to A^T . Also, all the analysis and results in this paper work on a complex A trivially with the transpose replaced by the conjugate transpose.

Throughout this paper, denote by $\|\cdot\|$ the 2-norm of a vector or matrix, by I_n the identity matrix of order n with n dropped whenever it is clear from the context, and by $\sigma_{\max}(X)$ and $\sigma_{\min}(X)$ the largest and smallest singular values of a matrix X , respectively.

2. PRELIMINARIES AND A BASIC ALGORITHM

Denote by

$$S = A^T A$$

the cross-product matrix of A . Let

$$A = U \begin{pmatrix} \Sigma \\ 0 \end{pmatrix} V^T$$

be the SVD of A with the diagonals σ 's of Σ being the singular values and the columns of U and V being the corresponding left and right singular vectors of A ;

see [8]. Then

$$(2.1) \quad V^T S V = \Sigma^2 \in \mathbb{R}^{n \times n}$$

is the eigendecomposition of S . We mention that at this moment we do not label the order of the singular values σ 's.

Given an interval $[a, b] \subset [\sigma_{\min}, \|A\|]$ with σ_{\min} being the smallest singular value $\sigma_{\min}(A)$ of A , suppose we are interested in all the singular values $\sigma \in [a, b]$ of A and/or the corresponding left and right singular vectors. Define

$$(2.2) \quad P_S = V_{in} V_{in}^T + \frac{1}{2} V_{ab} V_{ab}^T,$$

where V_{in} consists of the columns of V corresponding to the eigenvalues of S in the open interval (a^2, b^2) and V_{ab} consists of the columns of V corresponding to the eigenvalues of S that equal a^2 or b^2 . Notice that if neither of a nor b is a singular value of A , then $P_S = V_{in} V_{in}^T$ is the standard spectral projector of S associated with its eigenvalues $\sigma^2 \in [a^2, b^2]$. If either a or b or both them are singular values, then P_S is called a generalized spectral projector associated with all the $\sigma \in [a, b]$. The factor $\frac{1}{2}$ is necessary, and it corresponds to the step function to be introduced later that is approximated by the Chebyshev–Jackson series expansion in this paper or by a rational function in the context of the contour integral. In the sequel, for brevity we simply call P_S the spectral projector associated with $\sigma \in [a, b]$.

For an approximate singular triplet $(\hat{\sigma}, \hat{u}, \hat{v})$ of A , its absolute residual is

$$(2.3) \quad r = r(\hat{\sigma}, \hat{u}, \hat{v}) := \begin{bmatrix} A\hat{v} - \hat{\sigma}\hat{u} \\ A^T\hat{u} - \hat{\sigma}\hat{v} \end{bmatrix},$$

and the size of $\|r\|$ will be used to judge the convergence of $(\hat{\sigma}, \hat{u}, \hat{v})$ and design a stopping criterion.

Algorithm 1 is an algorithmic framework of our FEAST SVDSolver to be developed in this paper, where P is an approximation to P_S . It is a subspace iteration applied to P for computing the desired singular triplets of A and is an adaptation of the FEAST eigensolver to our SVD problem, where the right subspace is $\mathcal{K}^{(k)}$ and the left subspace $\mathcal{L}^{(k)} = A\mathcal{K}^{(k)}$. Line 7 mathematically realizes the Rayleigh–Ritz projection of S with respect to the subspace $\mathcal{K}^{(k)}$, that is, the $((\hat{\sigma}^{(k)})^2, \hat{v}^{(k)})$ are the Ritz pairs of S with respect to $\mathcal{K}^{(k)}$, and the corresponding $\hat{u}^{(k)} \in \mathcal{L}^{(k)}$ are the left Ritz vectors that approximate the left singular vectors of A associated with the desired singular values.

If $P = P_S$ defined by (2.2) and the subspace dimension $p = n_{sv}$, then under a certain mild condition on the initial subspace $\mathcal{S}^{(0)}$, Algorithm 1 finds the n_{sv} desired singular triplets in one iteration since $\mathcal{S}^{(1)} = \text{span}\{V_{in}, V_{ab}\}$ and $\mathcal{L}^{(1)}, \mathcal{K}^{(1)}$ are the exact left and right singular subspaces of A associated with all the $\sigma \in [a, b]$. We will focus on a number of issues on this algorithm in the sequel.

The following lemma is about how to estimate the trace of an implicit matrix. By *implicit* we mean that the matrix of interest is not available explicitly and only matrix–vector products for any appropriate vectors are available. The results are based on the Monte–Carlo simulation and are stated as follows [1, 3].

Lemma 2.1. *Let P be an $n \times n$ symmetric matrix. Define $H_M = \frac{1}{M} \sum_{i=1}^M z_i^T P z_i$, where the components z_{ij} of the random vectors z_i are independent and identically distributed Rademacher random variables, i.e., $\Pr(z_{ij} = 1) = \Pr(z_{ij} = -1) = \frac{1}{2}$.*

Algorithm 1 The basic FEAST SVDsolver: Subspace iteration on the approximate spectral projector P for the partial SVD of A .

- 1: **Input:** The interval $[a, b]$, the approximate spectral projector P , and a p -dimensional subspace $\mathcal{S}^{(0)}$ with $p \geq n_{sv}$.
- 2: **Output:** n_{sv} converged Ritz triplets $(\hat{\sigma}^{(k)}, \hat{u}^{(k)}, \hat{v}^{(k)})$.
- 3: $k = 0$.
- 4: **while** not converged **do**
- 5: $k \leftarrow k + 1$.
- 6: Form the projection subspace: $\mathcal{S}^{(k)} = P\mathcal{S}^{(k-1)}$, and construct the approximate right singular subspace $\mathcal{K}^{(k)} = \mathcal{S}^{(k)}$ and approximate left singular subspace $\mathcal{L}^{(k)} = A\mathcal{K}^{(k)}$.
- 7: The Rayleigh–Ritz projection: find $\hat{u}^{(k)} \in \mathcal{L}^{(k)}, \hat{v}^{(k)} \in \mathcal{K}^{(k)}, \hat{\sigma}^{(k)} \geq 0$ with $\|\hat{u}^{(k)}\| = \|\hat{v}^{(k)}\| = 1$ satisfying $A\hat{v}^{(k)} - \hat{\sigma}^{(k)}\hat{u}^{(k)} \perp \mathcal{L}^{(k)}, A^T\hat{u}^{(k)} - \hat{\sigma}^{(k)}\hat{v}^{(k)} \perp \mathcal{K}^{(k)}$.
- 8: Compute the residual norms (2.3) of Ritz triplets $(\hat{\sigma}^{(k)}, \hat{u}^{(k)}, \hat{v}^{(k)})$ for all the $\hat{\sigma}^{(k)} \in [a, b]$.
- 9: **end while**

Then the expectation $\mathbb{E}(H_M) = \text{tr}(P)$, variance $\text{Var}(H_M) = \frac{2}{M}(\|P\|_F^2 - \sum_{i=1}^n P_{ii}^2)$, and $\Pr(|H_M - \text{tr}(P)| \geq \epsilon) \leq \delta$ for $M \geq 8\epsilon^{-2}(\|P\|_F^2 + 2\epsilon\|P\|) \ln(\frac{2}{\delta})$.

Moreover, if P is positive semi-definite, then $\Pr(|H_M - \text{tr}(P)| \geq \epsilon \text{ tr}(P)) \leq \delta$ for $M \geq 8\epsilon^{-2}(1 + \epsilon) \ln(\frac{2}{\delta})\|P\|/\text{tr}(P)$.

From this lemma, we can see that the estimate for $|H_M - \text{tr}(P)|$ is absolute rather than relative error of $\text{tr}(P)$ when P is indefinite. This means that a reliable relative error estimate of $\text{tr}(P)$ depends on its size in the indefinite case. For the number n_{sv} of $\sigma \in [a, b]$, more appealing is relative error of $\text{tr}(P)$ in the context of the FEAST eigensolver and our FEAST SVDsolver as well as the SS-methods and its variants. The result in the lemma does not enable us to reliably estimate the trace $\text{tr}(P)$ when P is indefinite, which, in turn, makes us hard to reliably estimate the number of desired singular values in a given interval. Besides, for the same ϵ , though its implication is different in the indefinite and SPSD cases, the analysis and comparison in Remark 4 and Corollary 2 of [3] indicate that the sample number M needed for the indefinite case is proportional to $\|P\|_F^2$, the Frobenius norm of P , and could be n times larger than it is in the SPSD case for the same ϵ , meaning that an effective absolute error estimate may be much more costly.

As a matter of fact, we should distinguish the SPSD and indefinite cases and treat them separately. For P indefinite, a good choice of the absolute error bound ϵ depends critically on the size of the unknown $\text{tr}(P)$, and we have no way but empirically choose $\epsilon = \epsilon_1$ as some modest number rather than small, say $1 \sim 5$; but in the SPSD case, to make sense, we must choose a reasonably small relative error bound $\epsilon = \epsilon_2$, say 0.1, *independent* of the size of $\text{tr}(P)$. If we take $\epsilon_1 = \epsilon_2 \text{ tr}(P)$, the bounds for the corresponding sample numbers are almost the same. Unfortunately, this choice is impossible in practice since $\text{tr}(P)$ or a good estimate for it is unknown.

3. THE CHEBYSHEV–JACKSON SERIES EXPANSION OF A SPECIFIC STEP FUNCTION

For an interval $[a, b] \subset [-1, 1]$, let $h(x)$ be a step function defined by

$$(3.1) \quad h(x) = \begin{cases} 1, & x \in (a, b), \\ \frac{1}{2}, & x = a \text{ or } b, \\ 0, & x \in [-1, 1] \setminus [a, b], \end{cases}$$

where a and b are discontinuity points of $h(x)$, and $h(a) = h(b) = \frac{1}{2}$ equal the means

$$\frac{h(a+0) + h(a-0)}{2} = \frac{h(b+0) + h(b-0)}{2} = \frac{1}{2}.$$

Suppose that $h(x)$ is approximately expanded as the Chebyshev–Jackson polynomial series of degree d :

$$(3.2) \quad h(x) \approx \psi_d(x) = \frac{c_0}{2} + \sum_{j=1}^d \rho_{j,d} c_j T_j(x),$$

where $T_j(x)$ is the j -degree Chebyshev polynomial of the first kind [20]:

$$T_0(x) = 1, \quad T_1(x) = x, \quad T_{j+1}(x) = 2xT_j(x) - T_{j-1}(x), \quad j \geq 1,$$

the Fourier coefficients $c_j, j = 0, 1, \dots, d$, are

$$(3.3) \quad c_j = \begin{cases} \frac{2}{\pi}(\arccos(a) - \arccos(b)), & j = 0, \\ \frac{2}{\pi} \left(\frac{\sin(j \arccos(a)) - \sin(j \arccos(b))}{j} \right), & j > 0, \end{cases}$$

the Jackson damping factors $\rho_{j,d}$ are

$$(3.4) \quad \rho_{j,d} = 2 \sum_{\iota=0}^{d-j} t_\iota t_{\iota+j}, \quad j = 1, 2, \dots, d$$

with

$$(3.5) \quad t_\iota = \frac{\sin(\frac{\iota+1}{d+2}\pi)}{\sqrt{2 \sum_{\iota=0}^d \sin^2(\frac{\iota+1}{d+2}\pi)}}, \quad \iota = 0, 1, \dots, d.$$

It is shown in [5, 16] and [24, pp.20] that

$$(3.6) \quad \rho_{j,d} = \frac{(d+2-j) \sin(\frac{\pi}{d+2}) \cos(\frac{j\pi}{d+2}) + \cos(\frac{\pi}{d+2}) \sin(\frac{j\pi}{d+2})}{(d+2) \sin \frac{\pi}{d+2}}.$$

Define

$$(3.7) \quad g(\theta) = h(\cos \theta),$$

which is a function with period 2π . Then $g(\theta)$ is an even step function and

$$(3.8) \quad g(\theta) = \begin{cases} 1, & \theta \in (\beta, \alpha) \cup (-\alpha, -\beta), \\ \frac{1}{2}, & \theta \in \{-\alpha, -\beta, \beta, \alpha\}, \\ 0, & \theta \in [-\pi, \pi] \setminus ([\beta, \alpha] \cup [-\alpha, -\beta]), \end{cases}$$

where

$$\alpha = \arccos(a), \quad \beta = \arccos(b).$$

Let

$$(3.9) \quad q_d(\theta) = \frac{c_0}{2} + \sum_{j=1}^d \rho_{j,d} c_j \cos(j\theta).$$

Since $T_j(\cos \theta) = \cos(j\theta)$, by (3.2) we have

$$(3.10) \quad q_d(\theta) = \psi_d(\cos \theta).$$

Next we quantitatively analyze the pointwise convergence of $q_d(\theta)$ to $g(\theta)$. To this end, we need two lemmas.

Lemma 1.4 of [24, pp.17-18] shows that if $s(\theta)$ is continuous on $\theta \in [-\pi, \pi]$ and has period 2π then

$$\begin{aligned} & \frac{1}{2\pi} \int_{-\pi}^{\pi} s(\tau) d\tau + \sum_{j=1}^d \rho_{j,d} \left(\frac{\cos(j\theta)}{\pi} \int_{-\pi}^{\pi} s(\tau) \cos(j\tau) d\tau + \frac{\sin(j\theta)}{\pi} \int_{-\pi}^{\pi} s(\tau) \sin(j\tau) d\tau \right) \\ &= \frac{1}{\pi} \int_{-\pi}^{\pi} s(\tau + \theta) \left(\frac{1}{2} + \sum_{j=1}^d \rho_{j,d} \cos(j\tau) \right) d\tau. \end{aligned}$$

The above equality obviously holds when $s(\tau)$ is replaced by our step function $g(\theta)$ with period 2π . Therefore, we have

$$\begin{aligned} & \frac{1}{2\pi} \int_{-\pi}^{\pi} g(\tau) d\tau + \sum_{j=1}^d \rho_{j,d} \left(\frac{\cos(j\theta)}{\pi} \int_{-\pi}^{\pi} g(\tau) \cos(j\tau) d\tau + \frac{\sin(j\theta)}{\pi} \int_{-\pi}^{\pi} g(\tau) \sin(j\tau) d\tau \right) \\ &= \frac{1}{\pi} \int_{-\pi}^{\pi} g(\tau + \theta) \left(\frac{1}{2} + \sum_{j=1}^d \rho_{j,d} \cos(j\tau) \right) d\tau. \end{aligned}$$

Making use of (3.8) and the fact that $g(\theta)$ and $\sin(j\tau)$ are even and odd functions, respectively, we obtain

$$\frac{1}{\pi} \int_{-\pi}^{\pi} g(\tau) \cos(j\tau) d\tau = c_j, \quad \frac{1}{\pi} \int_{-\pi}^{\pi} g(\tau) \sin(j\tau) d\tau = 0, \quad j = 0, 1, \dots, d.$$

Consequently, we have proved the following lemma.

Lemma 3.1. *Let $g(\theta)$ and $q_d(\theta)$ be defined as (3.7) and (3.9), respectively. Then*

$$(3.11) \quad q_d(\theta) = \frac{1}{\pi} \int_{-\pi}^{\pi} g(\tau + \theta) u_d(\tau) d\tau,$$

where

$$u_d(\tau) = \frac{1}{2} + \sum_{j=1}^d \rho_{j,d} \cos(j\tau).$$

Lemma 3.2. *For $\theta \in \mathbb{R}$, it holds that $q_d(\theta) \in [0, 1]$.*

Proof. By (3.4), it is known from [24, pp.20] that

$$u_d(\tau) = \sum_{\iota=0}^d t_{\iota}^2 + \sum_{j=1}^d \left(\left(2 \sum_{\iota=0}^{d-j} t_{\iota} t_{\iota+j} \right) \cos(j\tau) \right) = \left(\sum_{\iota=0}^d t_{\iota} e^{i\iota\tau} \right) \left(\sum_{\iota=0}^d t_{\iota} e^{-i\iota\tau} \right) \geq 0,$$

where t_ι , $\iota = 0, 1, \dots, d$, are defined by (3.5), i is the imaginary unit, and e is the natural constant. Since $g(\theta)$ is also nonnegative, it follows from (3.11) that $q_d(\theta) \geq 0$. On the other hand,

$$(3.12) \quad \int_{-\pi}^{\pi} u_d(\tau) d\tau = \frac{1}{2} \int_{-\pi}^{\pi} d\tau + \sum_{j=1}^d \rho_{j,d} \int_{-\pi}^{\pi} \cos(j\tau) d\tau = \pi.$$

Therefore,

$$q_d(\theta) = \frac{1}{\pi} \int_{-\pi}^{\pi} g(\tau + \theta) u_d(\tau) d\tau \leq \frac{1}{\pi} \int_{-\pi}^{\pi} u_d(\tau) d\tau = 1.$$

□

In what follows we establish *quantitative* results on how fast $q_d(\theta)$ *pointwisely* converges to $g(\theta)$. Such kind of results is very appealing and plays a critical role in estimating accuracy of the approximate spectral projector \hat{P} to be constructed in terms of $\psi_d(x)$ and its eigenvalues, which will be used to analyze the convergence of the resulting FEAST SVDsolver and estimate the number n_{sv} of the desired $\sigma \in [a, b] \subset [\sigma_{\min}, \|A\|]$.

We first consider the pointwise convergence of $q_d(\theta)$ to $g(\theta)$ when $\theta \neq \alpha, \beta$.

Theorem 3.3. *Let $g(\theta)$ and $q_d(\theta)$ be defined as (3.7) and (3.9), respectively. For $\theta \in [0, \pi]$, $\theta \neq \alpha, \beta$ and $\alpha > \beta$, define*

$$\Delta_\theta = \min\{|\theta - \alpha|, |\theta - \beta|\}.$$

Then

$$(3.13) \quad |q_d(\theta) - g(\theta)| \leq \frac{\pi^4}{(2d+4)^2 \Delta_\theta^2}.$$

Proof. According to (3.7) and (3.8), we have

$$(3.14) \quad g(\tau) = g(\tau - 2\pi) = 0 \quad \text{for } \pi < \tau < 2\pi - \alpha.$$

For any given $\theta \in [0, \pi]$, define the function

$$F_\theta(\tau) = \begin{cases} \frac{g(\tau+\theta)-g(\theta)}{\tau^2}, & \tau \neq 0, \\ 0, & \tau = 0. \end{cases}$$

We classify $\theta \in [0, \pi]$ as $\theta \in [0, \beta)$, $\theta \in (\beta, \alpha)$ and $\theta \in (\alpha, \pi]$, and consider each case separately. Note that

$$\begin{cases} \text{if } \theta \in [0, \beta) \text{ then } \Delta_\theta = \beta - \theta \text{ and } \tau + \theta \in (-\beta, \beta) \text{ for } |\tau| < \Delta_\theta, \\ \text{if } \theta \in (\beta, \alpha) \text{ then } \Delta_\theta = \min\{\theta - \beta, \alpha - \theta\} \text{ and } \tau + \theta \in (\beta, \alpha) \text{ for } |\tau| < \Delta_\theta, \\ \text{if } \theta \in (\alpha, \pi] \text{ then } \Delta_\theta = \theta - \alpha \text{ and } \tau + \theta \in (\alpha, 2\pi - \alpha) \text{ for } |\tau| < \Delta_\theta. \end{cases}$$

Therefore, for any given $\theta \in [0, \pi]$ and $\theta \neq \alpha, \beta$, if $|\tau| < \Delta_\theta$, then by (3.8) we have $g(\tau + \theta) = g(\theta)$. As a result, we obtain

$$F_\theta(\tau) = 0 \quad \text{for } |\tau| < \Delta_\theta.$$

On the other hand, $|g(\tau + \theta) - g(\theta)| \leq 1$ means that

$$|F_\theta(\tau)| \leq \frac{1}{\Delta_\theta^2} \quad \text{for } |\tau| \geq \Delta_\theta.$$

Combining the above two results yields

$$|F_\theta(\tau)| \leq \frac{1}{\Delta_\theta^2} \quad \text{for } \tau \in \mathbb{R}.$$

Exploiting (3.12), we obtain

$$g(\theta) = \frac{1}{\pi} \int_{-\pi}^{\pi} g(\theta) u_d(\tau) d\tau.$$

Therefore,

$$\begin{aligned} (3.15) \quad |q_d(\theta) - g(\theta)| &= \left| \frac{1}{\pi} \int_{-\pi}^{\pi} (g(\tau + \theta) - g(\theta)) u_d(\tau) d\tau \right| \\ &\leq \frac{1}{\pi} \int_{-\pi}^{\pi} |F_\theta(\tau)| |\tau|^2 u_d(\tau) d\tau \\ &\leq \frac{1}{\pi} \int_{-\pi}^{\pi} \frac{|\tau|^2}{\Delta_\theta^2} u_d(\tau) d\tau. \end{aligned}$$

Making use of a result in [24, Section 1.1.2, pp.19-21] and (3.6) gives

$$(3.16) \quad \frac{1}{\pi} \int_{-\pi}^{\pi} |\tau|^2 u_d(\tau) d\tau \leq \frac{\pi}{2} \int_{-\pi}^{\pi} (1 - \cos(\tau)) u_d(\tau) d\tau = \frac{\pi^2}{2} (1 - \rho_{1,d}) \leq \frac{\pi^4}{(2d+4)^2}.$$

Therefore, it follows from this relation and (3.15) that

$$|q_d(\theta) - g(\theta)| \leq \frac{\pi^4}{(2d+4)^2 \Delta_\theta^2}.$$

□

The previous result requires that $\theta \neq \alpha, \beta$, the discontinuity points of the step function $g(\theta)$. If θ is equal to α or β , we need to make a special analysis and show how $q_d(\alpha)$ and $q_d(\beta)$ converge to $g(\alpha) = g(\beta) = \frac{1}{2}$.

Theorem 3.4. *Let $g(\theta)$ and $q_d(\theta)$ be defined as (3.7) and (3.9), respectively. Then for $\alpha, \beta \in (0, \pi)$ and $\alpha > \beta$ it holds that*

$$(3.17) \quad |q_d(\alpha) - g(\alpha)| \leq \frac{\pi^4}{2(2d+4)^2} \max \left\{ \frac{1}{(2\pi - 2\alpha)^2}, \frac{1}{(\alpha - \beta)^2} \right\},$$

$$(3.18) \quad |q_d(\beta) - g(\beta)| \leq \frac{\pi^4}{2(2d+4)^2} \max \left\{ \frac{1}{(2\beta)^2}, \frac{1}{(\alpha - \beta)^2} \right\}.$$

Proof. We first consider the case that $\theta = \alpha$. Define the functions

$$F_\alpha(\tau) = \begin{cases} \frac{g(\tau+\alpha)}{\tau^2}, & \tau > 0, \\ 0, & \tau = 0, \end{cases}$$

$$G_\alpha(\tau) = \begin{cases} \frac{g(\tau+\alpha)-1}{\tau^2}, & \tau < 0, \\ 0, & \tau = 0. \end{cases}$$

For $\tau \in (0, 2\pi - 2\alpha)$, we have $\tau + \alpha \in (\alpha, 2\pi - \alpha)$. Therefore, from (3.8) and (3.14), we obtain $g(\tau + \alpha) = 0$, showing that

$$F_\alpha(\tau) = 0 \quad \text{for } 0 < \tau < 2\pi - 2\alpha.$$

On the other hand, $0 \leq g(\tau + \alpha) \leq 1$ means that

$$0 \leq F_\alpha(\tau) \leq \frac{1}{(2\pi - 2\alpha)^2} \text{ for } \tau \geq 2\pi - 2\alpha.$$

Combining the above two results yields

$$0 \leq F_\alpha(\tau) \leq \frac{1}{(2\pi - 2\alpha)^2} \text{ for } \tau \geq 0.$$

For $\tau \in (\beta - \alpha, 0)$, we have $\tau + \alpha \in (\beta, \alpha)$. Therefore, from (3.8), we must have $g(\tau + \alpha) = 1$, i.e.,

$$G_\alpha(\tau) = 0 \text{ for } \beta - \alpha < \tau < 0.$$

On the other hand, $-1 \leq g(\tau + \alpha) - 1 \leq 0$ means that

$$-\frac{1}{(\alpha - \beta)^2} \leq G_\alpha(\tau) \leq 0 \text{ for } \tau \leq \beta - \alpha.$$

The above two results show that

$$-\frac{1}{(\alpha - \beta)^2} \leq G_\alpha(\tau) \leq 0 \text{ for } \tau \leq 0.$$

Since $u_d(\tau)$ is an even function and $\int_{-\pi}^{\pi} u_d(\tau) d\tau = \pi$ (cf. (3.12)), we have

$$\int_{-\pi}^0 u_d(\tau) d\tau = \int_0^\pi u_d(\tau) d\tau = \frac{\pi}{2}.$$

Therefore,

$$\begin{aligned} q_d(\alpha) - \frac{1}{2} &= \frac{1}{\pi} \int_{-\pi}^{\pi} g(\tau + \alpha) u_d(\tau) d\tau - \frac{1}{2} \\ &= \frac{1}{\pi} \int_0^\pi g(\tau + \alpha) u_d(\tau) d\tau + \frac{1}{\pi} \int_{-\pi}^0 g(\tau + \alpha) u_d(\tau) d\tau - \frac{1}{2} \\ &= \frac{1}{\pi} \int_0^\pi g(\tau + \alpha) u_d(\tau) d\tau + \frac{1}{\pi} \int_{-\pi}^0 (g(\tau + \alpha) - 1) u_d(\tau) d\tau \\ &= \frac{1}{\pi} \int_0^\pi F_\alpha(\tau) \tau^2 u_d(\tau) d\tau + \frac{1}{\pi} \int_{-\pi}^0 G_\alpha(\tau) \tau^2 u_d(\tau) d\tau. \end{aligned}$$

Exploiting (3.16), we obtain

$$\begin{aligned} 0 &\leq \frac{1}{\pi} \int_0^\pi F_\alpha(\tau) \tau^2 u_d(\tau) d\tau \leq \frac{1}{(2\pi - 2\alpha)^2} \frac{1}{\pi} \int_0^\pi \tau^2 u_d(\tau) d\tau \leq \frac{1}{(2\pi - 2\alpha)^2} \frac{\pi^4}{2(2d + 4)^2}, \\ 0 &\geq \frac{1}{\pi} \int_{-\pi}^0 G_\alpha(\tau) \tau^2 u_d(\tau) d\tau \geq -\frac{1}{(\alpha - \beta)^2} \frac{1}{\pi} \int_{-\pi}^0 \tau^2 u_d(\tau) d\tau \geq -\frac{1}{(\alpha - \beta)^2} \frac{\pi^4}{2(2d + 4)^2}, \end{aligned}$$

from which it follows that

$$\left| q_d(\alpha) - \frac{1}{2} \right| \leq \frac{\pi^4}{2(2d + 4)^2} \max \left\{ \frac{1}{(2\pi - 2\alpha)^2}, \frac{1}{(\alpha - \beta)^2} \right\},$$

that is, (3.17) holds by noticing that $g(\alpha) = \frac{1}{2}$.

Now we consider the case that $\theta = \beta$. Define the function

$$F_\beta(\tau) = \begin{cases} \frac{g(\tau + \beta) - 1}{\tau^2}, & \tau > 0, \\ 0, & \tau = 0, \end{cases}$$

$$G_\alpha(\tau) = \begin{cases} \frac{g(\tau+\beta)}{\tau^2}, & \tau < 0, \\ 0, & \tau = 0. \end{cases}$$

For $\tau \in (0, \alpha - \beta)$, we have $\tau + \beta \in (\beta, \alpha)$. Therefore, from (3.8), we have $g(\tau + \beta) = 1$, i.e.,

$$F_\beta(\tau) = 0 \text{ for } 0 < \tau < \alpha - \beta.$$

On the other hand, $-1 \leq g(\tau + \beta) - 1 \leq 0$ means that

$$-\frac{1}{(\alpha - \beta)^2} \leq F_\beta(\tau) \leq 0 \text{ for } \tau \geq \alpha - \beta.$$

Combining the above two results, we obtain

$$-\frac{1}{(\alpha - \beta)^2} \leq F_\beta(\tau) \leq 0 \text{ for } \tau \geq 0.$$

For $\tau \in (-2\beta, 0)$, we have $\tau + \beta \in (-\beta, \beta)$. Therefore, from (3.8), we have $g(\tau + \beta) = 0$, i.e.,

$$G_\beta(\tau) = 0 \text{ for } -2\beta < \tau < 0.$$

On the other hand, $0 \leq g(\tau + \beta) \leq 1$ means that

$$0 \leq G_\beta(\tau) \leq \frac{1}{(2\beta)^2} \text{ for } \tau \leq -2\beta.$$

The above two results show that

$$0 \leq G_\beta(\tau) \leq \frac{1}{(2\beta)^2} \text{ for } \tau \leq 0.$$

Since $\int_{-\pi}^0 u_d(\tau) d\tau = \int_0^\pi u_d(\tau) d\tau = \frac{\pi}{2}$, similarly to $q_d(\alpha) - \frac{1}{2}$, we have

$$\begin{aligned} q_d(\beta) - \frac{1}{2} &= \frac{1}{\pi} \int_{-\pi}^\pi g(\tau + \beta) u_d(\tau) d\tau - \frac{1}{2} \\ &= \frac{1}{\pi} \int_0^\pi F_\beta(\tau) \tau^2 u_d(\tau) d\tau + \frac{1}{\pi} \int_{-\pi}^0 G_\beta(\tau) \tau^2 u_d(\tau) d\tau. \end{aligned}$$

By (3.16), we have

$$\begin{aligned} 0 &\geq \frac{1}{\pi} \int_0^\pi F_\beta(\tau) \tau^2 u_d(\tau) d\tau \geq -\frac{1}{(\alpha - \beta)^2} \frac{1}{\pi} \int_0^\pi \tau^2 u_d(\tau) d\tau \geq -\frac{1}{(\alpha - \beta)^2} \frac{\pi^4}{2(2d+4)^2}, \\ 0 &\leq \frac{1}{\pi} \int_{-\pi}^0 G_\beta(\tau) \tau^2 u_d(\tau) d\tau \leq \frac{1}{(2\beta)^2} \frac{1}{\pi} \int_{-\pi}^0 \tau^2 u_d(\tau) d\tau \leq \frac{1}{(2\beta)^2} \frac{\pi^4}{2(2d+4)^2}. \end{aligned}$$

Therefore, we obtain

$$\left| q_d(\beta) - \frac{1}{2} \right| \leq \frac{\pi^4}{2(2d+4)^2} \max \left\{ \frac{1}{(2\beta)^2}, \frac{1}{(\alpha - \beta)^2} \right\},$$

which is (3.18) by noticing that $g(\beta) = \frac{1}{2}$. \square

By definition (3.2) of $\psi_d(x)$ and (3.10), Theorem 3.3 and Theorem 3.4 quantitatively shows how fast $\psi_d(x)$ *pointwisely* converges to $h(x)$ for $x \in [-1, 1]$ by taking $\theta = \arccos(x)$ and that the approximation accuracy of $q_d(\theta)$ to $g(\theta)$ is proportional to $\frac{1}{(2d+4)^2}$, that is, the convergence rate of $\psi_d(x)$ to $h(x)$ is as least as fast as $\frac{1}{(2d+4)^2}$ for $x \in [-1, 1]$. Furthermore, Theorem 3.3 shows that the convergence may be slow if Δ_θ is small, that is, θ is close to α or β or, equivalently, x is close to a or b ; Theorem 3.4 indicates that $q_d(\alpha)$ may converge to $g(\alpha)$ slowly if $\alpha \approx \pi$ or $\alpha \approx \beta$, that is,

$\psi_d(a)$ may converge to $h(a)$ slowly if $a \approx -1$ or $a \approx b$. Similarly, the convergence of $q_d(\beta)$ to $g(\beta)$ may be slow if $\beta \approx 0$ or $\alpha \approx \beta$, that is, the convergence of $\psi_d(b)$ to $h(b)$ may be slow if $b \approx 1$ or $a \approx b$.

4. THE FEAST SVDSOLVER BASED ON THE CROSS-PRODUCT MATRIX

4.1. Approximate spectral projector and its accuracy. We use the linear transformation

$$(4.1) \quad l(x) = \frac{2x - \|A\|^2 - \sigma_{\min}^2}{\|A\|^2 - \sigma_{\min}^2}$$

to map the spectrum interval $[\sigma_{\min}^2, \|A\|^2]$ of S to $[-1, 1]$. To use the transformation in computation, we need to estimate $\|A\|$ and σ_{\min} . We can run a Lanczos, i.e., Golub–Kahan, bidiagonalization type method on A several steps to estimate them [8, 17, 18]. For a given interval $[a, b] \subset [\sigma_{\min}, \|A\|]$, define the step function

$$h(x) = \begin{cases} 1, & x \in (l(a^2), l(b^2)), \\ \frac{1}{2}, & x = l(a^2) \text{ or } l(b^2), \\ 0, & x \in [-1, 1] \setminus [l(a^2), l(b^2)] \end{cases}$$

and the composite function

$$f(x) = h(l(x)),$$

so that

$$(4.2) \quad f(x) = \begin{cases} 1, & x \in (a^2, b^2), \\ \frac{1}{2}, & x = a^2 \text{ or } b^2, \\ 0, & x \in [\sigma_{\min}^2, \|A\|^2] \setminus [a^2, b^2]. \end{cases}$$

It follows from the above and (2.1) that the matrix function

$$(4.3) \quad f(S) = Vf(\Sigma^2)V^T = P_S,$$

where P_S is the spectral projector defined by (2.2).

When approximating $h(x)$ by the Chebyshev–Jackson series expansion $\psi_d(x)$ defined by (3.2), $\psi_d(l(x))$ is an approximation to $f(x)$ in (4.2). Correspondingly, in terms of it, we construct an approximate spectral projector

$$(4.4) \quad \hat{P} = \psi_d(l(S)) = \sum_{j=0}^d \rho_{j,d} c_j T_j(l(S)),$$

whose eigenvector matrix is V and eigenvalues are $\psi_d(l(\sigma_i^2))$ with $\sigma_i, i = 1, 2, \dots, n$ being the singular values of A . Based on the Fourier coefficients c_j and Jackson damping factors $\rho_{j,d}$ in section 3, we describe the construction of \hat{P} as Algorithm 2.

Remark 4.1. The unique action of \hat{P} in Algorithm 1 is to form matrix-matrix products. It suffices to store the coefficients $c_j, \rho_{j,d}, j = 0, \dots, d$ without forming \hat{P} explicitly. For convenience, c_0 in (4.4) corresponds to $\frac{c_0}{2}$ in (3.2).

Remark 4.2. The choice of d plays a key role in bounding the error $\|P_S - \hat{P}\|$, estimating n_{sv} and analyzing the convergence of Algorithm 4 to be proposed later, which is a detailed version of Algorithm 1.

Next we analyze the approximation accuracy $\|P_S - \hat{P}\|$ and estimate the eigenvalues $\psi_d(l(\sigma_i^2)), i = 1, 2, \dots, n$ of \hat{P} .

Algorithm 2 The construction of an approximate spectral projector \hat{P}

- 1: **Input:** The interval $[a, b]$, the estimates η and η_- for $\|A\|$ and σ_{\min} , and the series degree d .
- 2: **Output:** $c_j, \rho_{j,d}, j = 0, \dots, d$.
- 3: $l(x) = \frac{2x - \eta^2 - \eta_-^2}{\eta^2 - \eta_-^2}$.
- 4: $\hat{a} = l(a^2), \hat{b} = l(b^2)$.
- 5: $\alpha = \arccos(\hat{a}), \beta = \arccos(\hat{b})$.
- 6: $\zeta = \frac{\pi}{d+2}$.
- 7: **for** $j = 0, 1, \dots, d$ **do**
- 8: $c_j = \begin{cases} \frac{\alpha - \beta}{\pi}, & j = 0, \\ \frac{2 \sin(j\alpha) - \sin(j\beta)}{j}, & j > 0. \end{cases}$
- 9: $\rho_{j,d} = \frac{(d+2-j) \sin \zeta \cos(j\zeta) + \cos \zeta \sin(j\zeta)}{(d+2) \sin \zeta}$.
- 9: **end for**
- 10: $\hat{P} = \psi_d(l(S)) = \sum_{j=0}^d \rho_{j,d} c_j T_j(l(S))$.

Theorem 4.3. *Given the interval $[a, b] \subset [\sigma_{\min}, \|A\|]$, let*

$$\begin{aligned} \alpha &= \arccos(l(a^2)), \quad \beta = \arccos(l(b^2)), \\ \Delta_{il} &= |\arccos(l(\sigma_{il}^2)) - \alpha|, \quad \Delta_{ir} = |\arccos(l(\sigma_{ir}^2)) - \beta|, \\ \Delta_{ol} &= |\arccos(l(\sigma_{ol}^2)) - \alpha|, \quad \Delta_{or} = |\arccos(l(\sigma_{or}^2)) - \beta|, \end{aligned}$$

where σ_{il} , σ_{ir} and σ_{ol} , σ_{or} are the singular values of A that are the closest to a and b from inside and outside of $[a, b]$, respectively. Define

$$(4.5) \quad \Delta_{\min} = \min\{\Delta_{il}, \Delta_{ir}, \Delta_{ol}, \Delta_{or}\}.$$

Then

$$(4.6) \quad \|P_S - \hat{P}\| \leq \frac{\pi^4}{(2d+4)^2 \Delta_{\min}^2}.$$

Suppose that the singular values of A in $[a, b]$ are $\sigma_1, \dots, \sigma_{n_{sv}}$ with $\sigma_1, \dots, \sigma_r$ in (a, b) and $\sigma_{r+1}, \dots, \sigma_{n_{sv}}$ equal to the end a or b and that those in $[\sigma_{\min}, \|A\|] \setminus [a, b]$ are $\sigma_{n_{sv}+1}, \dots, \sigma_n$, and label $\psi_d(l(\sigma_i^2))$, $i = 1, 2, \dots, r$, $i = r+1, \dots, n_{sv}$ and $i = n_{sv}+1, \dots, n$ in decreasing order, respectively. Then if

$$(4.7) \quad d > \frac{\pi^2}{\Delta_{\min}} - 2,$$

it holds that

$$(4.8) \quad \|P_S - \hat{P}\| < \frac{1}{4}$$

and

$$(4.9) \quad \begin{aligned} 1 &\geq \psi_d(l(\sigma_1^2)) \geq \psi_d(l(\sigma_2^2)) \geq \dots \geq \psi_d(l(\sigma_r^2)) > \frac{3}{4} > \psi_d(l(\sigma_{r+1}^2)) \geq \dots \geq \psi_d(l(\sigma_{n_{sv}}^2)) \\ &> \frac{1}{4} > \psi_d(l(\sigma_{n_{sv}+1}^2)) \geq \dots \geq \psi_d(l(\sigma_n^2)) \geq 0. \end{aligned}$$

Proof. Note that the eigenvalues of P_S are

$$\begin{cases} f(\sigma_i^2) = h(l(\sigma_i^2)) = 1, & \sigma_i \in (a, b), \\ f(\sigma_i^2) = h(l(\sigma_i^2)) = \frac{1}{2}, & \sigma_i = a \text{ or } b, \\ f(\sigma_i^2) = h(l(\sigma_i^2)) = 0, & n_{sv} + 1 \leq i \leq n. \end{cases}$$

Then we obtain

$$\begin{aligned} \|P_S - \hat{P}\| &= \|f(S) - \psi_d(l(S))\| \\ &= \|f(\Sigma^2) - \psi_d(l(\Sigma^2))\| \\ &= \max_{i=1,2,\dots,n} |h(l(\sigma_i^2)) - \psi_d(l(\sigma_i^2))| \\ &= \max_{i=1,2,\dots,n} |h(\cos(\theta_i)) - \psi_d(\cos(\theta_i))|, \end{aligned}$$

where $\theta_i = \arccos(l(\sigma_i^2))$. Note that

$$\Delta_{\min} \leq \min\{2\pi - 2\alpha, \alpha - \beta, 2\beta\}.$$

It then follows from Theorem 3.3 and Theorem 3.4 that

$$\|P_S - \hat{P}\| \leq \frac{\pi^4}{(2d+4)^2 \Delta_{\min}^2},$$

which is (4.6) and indicates that $\hat{P} = \psi_d(l(S))$ converges to P_S as d increases. It is straightforward to justify from (4.6) that if d satisfies (4.7) then $\|P_S - \hat{P}\| < \frac{1}{4}$.

It is known from Lemma 3.2 that $\psi_d(l(\sigma_i^2))$, $i = 1, 2, \dots, n$ are in $[0, 1]$, meaning that \hat{P} is unconditionally SPSD. Therefore,

$$\|P_S - \hat{P}\| = \max \left\{ \max_{\sigma_i \in (a, b)} 1 - \psi_d(l(\sigma_i^2)), \max_{\sigma_i = a \text{ or } b} \left| \frac{1}{2} - \psi_d(l(\sigma_i^2)) \right|, \max_{i=n_{sv}+1, \dots, n} \psi_d(l(\sigma_i^2)) \right\}.$$

With condition (4.7), the above relation shows that

$$\begin{aligned} 0 \leq 1 - \psi_d(l(\sigma_i^2)) &< \frac{1}{4}, \quad \sigma_i \in (a, b), \\ \left| \frac{1}{2} - \psi_d(l(\sigma_i^2)) \right| &< \frac{1}{4}, \quad \sigma_i = a \text{ or } b, \\ 0 \leq \psi_d(l(\sigma_i^2)) &< \frac{1}{4}, \quad i = n_{sv} + 1, \dots, n, \end{aligned}$$

indicating that

$$\begin{aligned} \frac{3}{4} < \psi_d(l(\sigma_i^2)) &\leq 1, \quad \sigma_i \in (a, b), \\ \frac{1}{4} < \psi_d(l(\sigma_i^2)) &< \frac{3}{4}, \quad \sigma_i = a \text{ or } b. \end{aligned}$$

With the labeling order of $\psi_d(l(\sigma_i^2))$, $i = 1, 2, \dots, n$, the above proves (4.9). \square

Remark 4.4. For d fixed, \hat{P} better approximates P_S for Δ_{\min} larger. As d increases, $\psi_d(l(\sigma_i^2)) \approx 1$, $i = 1, 2, \dots, r$, $\psi_d(l(\sigma_i^2)) \approx \frac{1}{2}$, $i = r+1, \dots, n_{sv}$, and $\psi_d(l(\sigma_i^2)) \approx 0$, $i = n_{sv}+1, \dots, n$. In fact, it follows from (4.6) that we can make $\|P_S - \hat{P}\| < \epsilon$

with ϵ arbitrarily small by increasing d . In this case, we have

$$(4.10) \quad 1 - \epsilon < \psi_d(l(\sigma_i^2)) \leq 1, i = 1, 2, \dots, r,$$

$$(4.11) \quad \frac{1}{2} - \epsilon < \psi_d(l(\sigma_i^2)) < \frac{1}{2} + \epsilon, i = r + 1, \dots, n_{sv},$$

$$(4.12) \quad 0 \leq \psi_d(l(\sigma_i^2)) < \epsilon, i = n_{sv} + 1, \dots, n.$$

4.2. Estimates for the number of desired singular values. Note that $\text{tr}(P_S) = r + \frac{n_{sv} - r}{2} = \frac{r + n_{sv}}{2}$, which equals n_{sv} when none of a and b is a singular value of A . We now estimate n_{sv} in order to make the subspace dimension $p \geq n_{sv}$ in Algorithm 1. Since \hat{P} is SPSD, we can exploit Lemma 2.1 to derive a reliable estimate of the trace $\text{tr}(\hat{P})$ and use it as an approximation of $\text{tr}(P_S)$.

Theorem 4.5. *The trace $\text{tr}(\hat{P})$ of the approximate spectral projector \hat{P} satisfies*

$$(4.13) \quad |\text{tr}(P_S) - \text{tr}(\hat{P})| \leq \frac{n\pi^4}{(2d+4)^2\Delta_{\min}^2}.$$

Define $\hat{H}_M = \frac{1}{M} \sum_{i=1}^M z_i^T \hat{P} z_i$, where the components z_{ij} of the random vectors z_i are independent and identically distributed Rademacher random variables. Then for $M \geq 8\epsilon^{-2}(1+\epsilon)\ln(\frac{2}{\delta})\|\hat{P}\|/\text{tr}(\hat{P})$ it holds that

$$(4.14) \quad \Pr(|\hat{H}_M - \text{tr}(\hat{P})| \geq \epsilon \text{tr}(\hat{P})) \leq \delta.$$

Proof. Since

$$(4.15) \quad \begin{aligned} |\text{tr}(P_S) - \text{tr}(\hat{P})| &= \left| \sum_{i=1}^n (f(\sigma_i^2) - \psi_d(l(\sigma_i^2))) \right| \\ &\leq \sum_{i=1}^n |f(\sigma_i^2) - \psi_d(l(\sigma_i^2))| \\ &\leq n \max_{i=1,2,\dots,n} |f(\sigma_i^2) - \psi_d(l(\sigma_i^2))| \end{aligned}$$

$$(4.16) \quad = n\|P_S - \hat{P}\|,$$

by (4.6) we have

$$|\text{tr}(P_S) - \text{tr}(\hat{P})| \leq \frac{n\pi^4}{(2d+4)^2\Delta_{\min}^2},$$

which is (4.13).

Since \hat{P} is SPSD, by Lemma 2.1, for $M \geq 8\epsilon^{-2}(1+\epsilon)\ln(\frac{2}{\delta})\frac{\|\hat{P}\|}{\text{tr}(\hat{P})}$ we have

$$\Pr(|\hat{H}_M - \text{tr}(\hat{P})| \geq \epsilon \text{tr}(\hat{P})) \leq \delta.$$

□

Remark 4.6. Theorem 4.5 indicates that the smallest sample number $M \approx \frac{8\ln\frac{2}{\delta}}{\epsilon^2 n_{sv}}$. Note that a reasonably small $\epsilon \in [10^{-2}, 10^{-1}]$ means that \hat{H}_M is a reliable estimate for $\text{tr}(\hat{P})$ with high probability $1 - \delta \approx 1$ for $\delta \sim 10^{-2}$. For n_{sv} ranging from a few to around one thousand, a modest M generally gives a reliable estimate for $\text{tr}(\hat{P})$. Surprisingly, the bigger n_{sv} is, the smaller M is needed to give the same accuracy ϵ for a fixed δ .

Remark 4.7. Since $\text{tr}(P_S) = \frac{n_{sv}+r}{2}$, bound in (4.13) makes sense, that is, the bound is smaller than $\text{tr}(P_S)$ itself, only when

$$(4.17) \quad d \geq \frac{\pi^2}{\Delta_{\min}} \sqrt{\frac{n}{2(n_{sv}+r)}} - 2,$$

which requires that d be large. However, we should remind that bound (4.13) is generally pessimistic since bound (4.15) and thus bound (4.16) may be a considerable overestimate by noticing that the signs of $f(\sigma_i^2) - \psi_d(l(\sigma_i^2)) = 1 - \psi_d(l(\sigma_i^2)) \geq 0$, $i = 1, 2, \dots, r$ and $f(\sigma_i^2) - \psi_d(l(\sigma_i^2)) = -\psi_d(l(\sigma_i^2)) \leq 0$, $i = n_{sv} + 1, \dots, n$ are opposite, and their sizes may differ considerably. As a result, the factor n in bounds (4.13) and (4.16) may actually behave like $\mathcal{O}(1)$, which means that $|\text{tr}(P_S) - \text{tr}(\hat{P})| \approx \|P_S - \hat{P}\|$, and condition (4.17) on d is generally too stringent due to the pessimistic bound (4.13), where the conservative large factor n may resemble $\mathcal{O}(1)$. Consequently, $\text{tr}(\hat{P})$ can be a good estimate for $\text{tr}(P_S) = \frac{n_{sv}+r}{2}$ for $d \sim \frac{\pi^2}{\Delta_{\min}\sqrt{2(n_{sv}+r)}} = \frac{\pi^2}{2\Delta_{\min}\sqrt{n_{sv}}}$ when $n_{sv} = r$. Combining this with (4.14) and its condition on M , we conclude that $\text{tr}(\hat{P})$ is practically a good estimate for $\text{tr}(P_S)$ when M is modest and $d \sim \frac{\pi^2}{2\Delta_{\min}\sqrt{n_{sv}}}$.

Extensive numerical experiments have demonstrated that

$$(4.18) \quad p = \lceil \mu \hat{H}_M \rceil \in [\lceil 1.1 \hat{H}_M \rceil, \lceil 1.5 \hat{H}_M \rceil]$$

is a reliable and practical choice, where $\lceil \cdot \rceil$ is the ceil function. This selection strategy guarantees that $p \geq n_{sv}$ in all the numerical experiments of section 6. In fact, we have $|\hat{H}_M - \text{tr}(\hat{P})| \leq \epsilon \text{tr}(\hat{P})$ with the high probability $1 - \delta \approx 1$ for a modest M . Therefore, $\hat{H}_M \geq (1 - \epsilon) \text{tr}(\hat{P})$ and $\mu \hat{H}_M \geq \mu(1 - \epsilon) \text{tr}(\hat{P})$. Obviously, $\mu = 1.1$ ensures that $\mu(1 - \epsilon) \geq 1$ with $\epsilon \leq \frac{1}{11}$, and $\mu = 1.5$ ensures that $\mu(1 - \epsilon) \geq 1$ with $\epsilon \leq \frac{1}{3}$. As a result, p in (4.18) is a reliable upper bound for $\text{tr}(\hat{P})$ provided that M is reasonably large. The bigger M is, the smaller ϵ in (4.14) is, so that p in (4.18) is further bigger than n_{sv} .

Based on the above description, we now present Algorithm 3 to determine the subspace dimension p .

Algorithm 3 Determination of subspace dimension p

- 1: **Input:** $c_j, \rho_{j,d}, j = 0, \dots, d, \eta, \eta_-$, and M Rademacher random n -vectors z_1, z_2, \dots, z_M .
- 2: **Output:** p .
- 3: Compute $\hat{H}_M = \frac{1}{M} \sum_{i=1}^M z_i^T \hat{P} z_i = \frac{1}{M} \sum_{i=1}^M \sum_{j=0}^d \rho_{j,d} c_j z_i^T T_j(l(S)) z_i$.
- 4: Choose p by (4.18).

4.3. A cross-product FEAST SVDSolver using the Chebyshev–Jackson series expansion. Having determined the approximate spectral projector \hat{P} by Algorithm 2 and the subspace dimension p by Algorithm 3, we apply Algorithm 1 to \hat{P} , form an approximate eigenspace of \hat{P} associated with its p dominant eigenvalues $\psi_d(l(\sigma_i^2))$, $i = 1, 2, \dots, p$, and compute its orthonormal basis using the QR factorization at each iteration. We then take the current subspace as the right projection subspace $\mathcal{K}^{(k)}$, form the left projection subspace $\mathcal{L}^{(k)} = A\mathcal{K}^{(k)}$, and

project A onto them to compute Ritz approximations $(\hat{\sigma}_j^{(k)}, \hat{u}_j^{(k)}, \hat{v}_j^{(k)})$ of the desired n_{sv} singular triplets (σ_j, u_j, v_j) , $j = 1, 2, \dots, n_{sv}$. We describe the procedure as Algorithm 4.

Algorithm 4 The cross-product based SVDsolver using the Chebyshev–Jackson series

- 1: **Input:** The interval $[a, b]$, $c_j, \rho_{j,d}, j = 0, \dots, d, \eta, \eta_-, p$, and an n -by- p column orthonormal matrix $\hat{V}^{(0)}$ with $p \geq n_{sv}$.
- 2: **Output:** The n_{sv} converged Ritz triplets $(\hat{\sigma}_j^{(k)}, \hat{u}_j^{(k)}, \hat{v}_j^{(k)})$ with $\hat{\sigma}_j^{(k)} \in [a, b]$.
- 3: **for** $k = 1, 2, \dots$, **do**
- 4: Compute $Y^{(k)} = \hat{P}\hat{V}^{(k-1)} = \sum_{j=0}^d \rho_{j,d} c_j T_j(l(S)) \hat{V}^{(k-1)}$ and $Z^{(k)} = AY^{(k)}$.
- 5: Make QR factorizations: $Y^{(k)} = Q_1^{(k)} R_1^{(k)}$ and $Z^{(k)} = Q_2^{(k)} R_2^{(k)}$.
- 6: Compute the projection matrix: $\bar{A}^{(k)} = (Q_2^{(k)})^T A Q_1^{(k)}$.
- 7: Compute the SVD: $\bar{A}^{(k)} = \bar{U}^{(k)} \hat{\Sigma}^{(k)} (\bar{V}^{(k)})^T$ with $\hat{\Sigma}^{(k)} = \text{diag}(\hat{\sigma}_1^{(k)}, \dots, \hat{\sigma}_p^{(k)})$.
- 8: Form $\hat{U}^{(k)} = Q_2^{(k)} \bar{U}^{(k)}$ and $\hat{V}^{(k)} = Q_1^{(k)} \bar{V}^{(k)}$.
- 9: Select those $\hat{\sigma}_j^{(k)} \in [a, b]$, compute the residual norms of $(\hat{\sigma}_j^{(k)}, \hat{u}_j^{(k)}, \hat{v}_j^{(k)})$, where $\hat{u}_j^{(k)} = \hat{U}^{(k)} e_j$ and $\hat{v}_j^{(k)} = \hat{V}^{(k)} e_j$ with e_j being column j of I_p , and test convergence.
- 10: **end for**

Next we make a convergence analysis on Algorithm 4.

Write $\gamma_i = \psi_d(l(\sigma_i^2))$, $i = 1, 2, \dots, n$, and suppose that $p \geq n_{sv}$. Recall from (2.1) that the columns of V are the right singular vectors of A . We partition $V = [V_p, V_{p,\perp}]$ and set up the following notation:

$$(4.19) \quad V_p = [v_1, \dots, v_p], \quad V_{p,\perp} = [v_{p+1}, \dots, v_n],$$

$$(4.20) \quad \Gamma_p = \text{diag}(\gamma_1, \dots, \gamma_p), \quad \Gamma'_p = \text{diag}(\gamma_{p+1}, \dots, \gamma_n),$$

$$(4.21) \quad \Sigma_p = \text{diag}(\sigma_1, \dots, \sigma_p), \quad \Sigma'_p = \text{diag}(\sigma_{p+1}, \dots, \sigma_n).$$

Note that Algorithm 4 generates the subspaces

$$\text{span}\{\hat{V}^{(k)}\} = \text{span}\{Q_1^{(k)}\} = \text{span}\{Y^{(k)}\} = \hat{P}\text{span}\{\hat{V}^{(k-1)}\},$$

showing that

$$\text{span}\{\hat{V}^{(k)}\} = \hat{P}^k \text{span}\{\hat{V}^{(0)}\}.$$

We can establish the following convergence results on $\text{span}\{Q_1^{(k)}\}$ and the Ritz values $\hat{\sigma}_i^{(k)}$ computed by Algorithm 4.

Theorem 4.8. *Suppose that $\gamma_p > \gamma_{p+1}$ and $V_p^T \hat{V}^{(0)}$ is invertible. Then*

$$(4.22) \quad Q_1^{(k)} = (V_p + V_{p,\perp} E^{(k)})(M^{(k)})^{-\frac{1}{2}} U^{(k)}$$

with

$$(4.23) \quad E^{(0)} = V_{p,\perp}^T \hat{V}^{(0)} (V_p^T \hat{V}^{(0)})^{-1}, \quad E^{(k)} = \Gamma_p'^k E^{(0)} \Gamma_p^{-k},$$

$$(4.24) \quad M^{(k)} = I + (E^{(k)})^T E^{(k)}$$

and $U^{(k)}$ being an orthogonal matrix,

$$(4.25) \quad \|E^{(k)}\| \leq \left(\frac{\gamma_{p+1}}{\gamma_p}\right)^k \|E^{(0)}\|,$$

and the distance between $\text{span}\{Q_1^{(k)}\}$ and $\text{span}\{V_p\}$ (cf. [8, pp.82]) satisfies

$$(4.26) \quad \text{dist}(\text{span}\{Q_1^{(k)}\}, \text{span}\{V_p\}) = \frac{\|E^{(k)}\|}{\sqrt{1 + \|E^{(k)}\|^2}} \leq \left(\frac{\gamma_{p+1}}{\gamma_p}\right)^k \|E^{(0)}\|.$$

Label $\hat{\sigma}_1^{(k)}, \dots, \hat{\sigma}_p^{(k)}$ in the same order as $\sigma_1, \dots, \sigma_p$ in Theorem 4.3. Then

$$(4.27) \quad |(\hat{\sigma}_i^{(k)})^2 - \sigma_i^2| \leq \|A\|^2 \left(2 \left(\frac{\gamma_{p+1}}{\gamma_p}\right)^{2k} + \left(\frac{\gamma_{p+1}}{\gamma_p}\right)^{4k} \|E^{(0)}\|^2 \right) \|E^{(0)}\|^2, \quad i = 1, 2, \dots, n_{sv}.$$

Proof. Expand $\hat{V}^{(0)}$ as the orthogonal direct sum of V_p and $V_{p,\perp}$. Then

$$\begin{aligned} \hat{V}^{(0)} &= V_p V_p^T \hat{V}^{(0)} + V_{p,\perp} V_{p,\perp}^T \hat{V}^{(0)} \\ &= (V_p + V_{p,\perp} V_{p,\perp}^T \hat{V}^{(0)} (V_p^T \hat{V}^{(0)})^{-1}) V_p^T \hat{V}^{(0)}, \end{aligned}$$

from which and the first relation in (4.23) it follows that

$$\hat{V}^{(0)} (V_p^T \hat{V}^{(0)})^{-1} = V_p + V_{p,\perp} E^{(0)}.$$

From $\hat{P}V_p = V_p \Gamma_p$ and $\hat{P}V_{p,\perp} = V_{p,\perp} \Gamma_p'$, we obtain $\hat{P}^k V_p = V_p \Gamma_p^k$ and $\hat{P}^k V_{p,\perp} = V_{p,\perp} \Gamma_p'^k$. Therefore,

$$(4.28) \quad \begin{aligned} \hat{P}^k \hat{V}^{(0)} (V_p^T \hat{V}^{(0)})^{-1} \Gamma_p^{-k} &= V_p + \hat{P}^k V_{p,\perp} E^{(0)} \Gamma_p^{-k} \\ &= V_p + V_{p,\perp} \Gamma_p'^k E^{(0)} \Gamma_p^{-k} = V_p + V_{p,\perp} E^{(k)} \end{aligned}$$

with $E^{(k)}$ defined as in (4.23). Obviously,

$$\|E^{(k)}\| \leq \left(\frac{\gamma_{p+1}}{\gamma_p}\right)^k \|E^{(0)}\| \rightarrow 0,$$

which is (4.25).

By (4.28), we obtain

$$\text{span}\{Q_1^{(k)}\} = \hat{P}^k \text{span}\{\hat{V}^{(0)}\} = \hat{P}^k \text{span}\{\hat{V}^{(0)} (V_p^T \hat{V}^{(0)})^{-1} \Gamma_p^{-k}\} = \text{span}\{V_p + V_{p,\perp} E^{(k)}\}.$$

As a result, since $Q_1^{(k)}$ is column orthonormal, we can express $Q_1^{(k)}$ as

$$Q_1^{(k)} = (V_p + V_{p,\perp} E^{(k)}) (M^{(k)})^{-\frac{1}{2}} U^{(k)},$$

which establishes (4.22), where

$$M^{(k)} = (V_p + V_{p,\perp} E^{(k)})^T (V_p + V_{p,\perp} E^{(k)}) = I + (E^{(k)})^T E^{(k)}$$

is the matrix in (4.24) and $U^{(k)}$ is an orthogonal matrix.

By the distance definition [8, pp.82] of two subspaces, from (4.22) we have

$$\begin{aligned} \text{dist}(\text{span}\{Q_1^{(k)}\}, \text{span}\{V_p\}) &= \|V_{p,\perp}^T Q_1^{(k)}\| = \|E^{(k)} (M^{(k)})^{-1/2} U^{(k)}\| \\ &= \|E^{(k)} (M^{(k)})^{-1/2}\| = \frac{\|E_k\|}{\sqrt{1 + \|E_k\|^2}}, \end{aligned}$$

which, together with (4.25), proves (4.26).

Since $(E^{(k)})^T E^{(k)}$ is SPSD, from the form (4.24) of $M^{(k)}$ we can write

$$(M^{(k)})^{1/2} = I + F^{(k)}.$$

Note that the eigenvalues of $M^{(k)}$ are larger than one, so are the eigenvalues of $(M^{(k)})^{1/2}$. Therefore, $F^{(k)}$ is SPSD too, so is $(F^{(k)})^2$. On the other hand, from $M^{(k)} = (I + F^{(k)})^2$ and (4.24) we obtain

$$(E^{(k)})^T E^{(k)} = 2F^{(k)} + (F^{(k)})^2,$$

i.e.,

$$(E^{(k)})^T E^{(k)} - (F^{(k)})^2 = 2F^{(k)}.$$

Since $(F^{(k)})^2$ is SPSD, the eigenvalues of $2F^{(k)}$ are no more than the corresponding ones of $(E^{(k)})^T E^{(k)}$ in the same labeling order, which particularly means that

$$2\|F^{(k)}\| \leq \|(E^{(k)})^T E^{(k)}\| = \|E^{(k)}\|^2.$$

Therefore,

$$\begin{aligned} \|\Sigma_p^2 - (M^{(k)})^{1/2} \Sigma_p^2 (M^{(k)})^{1/2}\| &= \|\Sigma_p^2 - (I + F^{(k)}) \Sigma_p^2 (I + F^{(k)})\| \\ &= \|\Sigma_p^2 F^{(k)} + F^{(k)} \Sigma_p^2 + F^{(k)} \Sigma_p^2 F^{(k)}\| \\ (4.29) \quad &\leq \|\Sigma_p^2\| \|E^{(k)}\|^2 + \|\Sigma_p^2\| \|E^{(k)}\|^4. \end{aligned}$$

Exploiting the eigendecomposition $S = V \Sigma^2 V^T$, (4.22) and (4.29) and noticing that $\|(M^{(k)})^{-1/2}\| \leq 1$, we obtain

$$\begin{aligned} &\|U^{(k)}(Q_1^{(k)})^T S Q_1^{(k)}(U^{(k)})^T - \Sigma_p^2\| \\ &= \|(M^{(k)})^{-1/2}(V_p^T + (E^{(k)})^T V_{p,\perp}^T) V \Sigma^2 V^T (V_p + V_{p,\perp} E^{(k)}) (M^{(k)})^{-1/2} - \Sigma_p^2\| \\ &= \|(M^{(k)})^{-1/2}(\Sigma_p^2 + (E^{(k)})^T (\Sigma_p')^2 E^{(k)}) (M^{(k)})^{-1/2} - \Sigma_p^2\| \\ &= \|(M^{(k)})^{-1/2}(\Sigma_p^2 - (M^{(k)})^{1/2} \Sigma_p^2 (M^{(k)})^{1/2} + (E^{(k)})^T (\Sigma_p')^2 E^{(k)}) (M^{(k)})^{-1/2}\| \\ &\leq \|\Sigma_p^2 - (M^{(k)})^{1/2} \Sigma_p^2 (M^{(k)})^{1/2}\| + \|(E^{(k)})^T (\Sigma_p')^2 E^{(k)}\| \\ &= \|\Sigma_p^2\| \|E^{(k)}\|^2 + \|\Sigma_p^2\| \|E^{(k)}\|^4 + \|(E^{(k)})^T (\Sigma_p')^2 E^{(k)}\| \\ &\leq 2\|A\|^2 \|E^{(k)}\|^2 + \|A\|^2 \|E^{(k)}\|^4, \end{aligned}$$

where we have used $\|(E^{(k)})^T (\Sigma_p')^2 E^{(k)}\| \leq \|A\|^2 \|E^{(k)}\|^2$. Since the eigenvalues of $U^{(k)}(Q_1^{(k)})^T S Q_1^{(k)}(U^{(k)})^T$ are $(\hat{\sigma}_i^{(k)})^2$, $i = 1, 2, \dots, p$, by a standard perturbation result [30, Theorem 3.8, pp.42], the above relation and (4.25) lead to (4.27). \square

The following theorem establishes convergence results on the Ritz vectors $\hat{u}_i^{(k)}$ and $\hat{v}_i^{(k)}$ and a new convergence result on the Ritz values $\hat{\sigma}_i^{(k)}$.

Theorem 4.9. *Let*

$$\beta^{(k)} = \|P^{(k)} S(I - P^{(k)})\|,$$

where $P^{(k)}$ is the orthogonal projector onto $\text{span}\{Q_1^{(k)}\}$. Assume that each singular value of A in $[a, b]$ is simple, and define

$$\delta_i^{(k)} = \min_{j \neq i} |\sigma_i^2 - (\hat{\sigma}_j^{(k)})^2|, \quad i = 1, 2, \dots, n_{sv}.$$

Then for $i = 1, 2, \dots, n_{sv}$ it holds that

$$(4.30) \quad \sin \angle(\hat{v}_i^{(k)}, v_i) \leq \sqrt{1 + \frac{(\beta^{(k)})^2}{(\delta_i^{(k)})^2}} \left(\frac{\gamma_{p+1}}{\gamma_i} \right)^k \|E^{(0)}\|,$$

$$(4.31) \quad \sin \angle(\hat{u}_i^{(k)}, u_i) \leq \frac{\|A\|}{\hat{\sigma}_i^{(k)}} \sqrt{1 + \frac{(\beta^{(k)})^2}{(\delta_i^{(k)})^2}} \left(\frac{\gamma_{p+1}}{\gamma_i} \right)^k \|E^{(0)}\|,$$

$$(4.32) \quad |\hat{\sigma}_i^{(k)} - \sigma_i| \leq \frac{\|A\|^2}{\hat{\sigma}_i^{(k)} + \sigma_i} \left(1 + \frac{(\beta^{(k)})^2}{(\delta_i^{(k)})^2} \right) \left(\frac{\gamma_{p+1}}{\gamma_i} \right)^{2k} \|E^{(0)}\|^2.$$

Proof. Note that $((\hat{\sigma}_i^{(k)})^2, \hat{v}_i^{(k)})$, $i = 1, 2, \dots, n_{sv}$ are the Ritz pairs of S with respect to $\text{span}\{Q_1^{(k)}\}$. Applying [27, Theorem 4.6, Proposition 4.5] to our case yields

$$(4.33) \quad \sin \angle(\hat{v}_i^{(k)}, v_i) \leq \sqrt{1 + \frac{(\beta^{(k)})^2}{(\delta_i^{(k)})^2}} \sin \angle(v_i, \text{span}\{Q_1^{(k)}\}),$$

$$(4.34) \quad |(\hat{\sigma}_i^{(k)})^2 - \sigma_i^2| \leq \|S - \sigma_i^2 I\| \sin^2 \angle(\hat{v}_i^{(k)}, v_i) \leq \|A\|^2 \sin^2 \angle(\hat{v}_i^{(k)}, v_i).$$

From (4.22) and (4.20), we obtain

$$\begin{aligned} \sin \angle(v_i, \text{span}\{Q_1^{(k)}\}) &= \sin \angle(v_i, \text{span}\{Q_1^{(k)}(U^{(k)})^T(M^{(k)})^{1/2}\}) \\ &= \sin \angle(v_i, V_p + V_{p,\perp} E^{(k)}) \\ &\leq \sin \angle(v_i, v_i + V_{p,\perp} E^{(k)} e_i) \\ &= \frac{\|E^{(k)} e_i\|}{\sqrt{1 + \|E^{(k)} e_i\|^2}} \\ &\leq \|E^{(k)} e_i\| = \|\Gamma_p'^k E^{(0)} \Gamma_p^{-k} e_i\| \leq \|\Gamma_p'^k E^{(0)}\| \gamma_i^{-k} \\ &\leq \left(\frac{\gamma_{p+1}}{\gamma_i} \right)^k \|E^{(0)}\|. \end{aligned}$$

Substituting the last inequality into (4.33) and (4.34) gives

$$\begin{aligned} \sin \angle(\hat{v}_i^{(k)}, v_i) &\leq \sqrt{1 + \frac{(\beta^{(k)})^2}{(\delta_i^{(k)})^2}} \left(\frac{\gamma_{p+1}}{\gamma_i} \right)^k \|E^{(0)}\|, \\ |(\hat{\sigma}_i^{(k)})^2 - \sigma_i^2| &\leq \|A\|^2 \left(1 + \frac{(\beta^{(k)})^2}{(\delta_i^{(k)})^2} \right) \left(\frac{\gamma_{p+1}}{\gamma_i} \right)^{2k} \|E^{(0)}\|^2, \end{aligned}$$

which proves (4.30) and (4.32).

In terms of the notation in Steps 7–9 of Algorithm 4, we obtain

$$\hat{U}^{(k)} \hat{\Sigma}^{(k)} = Q_2^{(k)} \bar{U}^{(k)} \hat{\Sigma}^{(k)} = A Q_1^{(k)} \bar{V}^{(k)} = A \hat{V}^{(k)},$$

showing that

$$(4.35) \quad A \hat{v}_i^{(k)} = \hat{\sigma}_i^{(k)} \hat{u}_i^{(k)}.$$

Decompose $\hat{v}_i^{(k)}$ into the orthogonal direct sum:

$$\hat{v}_i^{(k)} = v_i \cos \angle(\hat{v}_i^{(k)}, v_i) + z \sin \angle(\hat{v}_i^{(k)}, v_i),$$

where z is orthogonal to v_i with $\|z\| = 1$. Abbreviate $\angle(\hat{v}_i^{(k)}, v_i)$ as ϕ_i . Then

$$(4.36) \quad \hat{\sigma}_i^{(k)} \hat{u}_i^{(k)} = A \hat{v}_i^{(k)} = A(v_i \cos \phi_i + z \sin \phi_i) = \sigma_i u_i \cos \phi_i + A z \sin \phi_i.$$

Since

$$u_i^T A z = z^T A^T u_i = \sigma_i z^T v_i = 0,$$

it follows from (4.36) that

$$(4.37) \quad \sin \angle(\hat{u}_i^{(k)}, u_i) = \frac{\|A z\|}{\hat{\sigma}_i^{(k)}} \sin \phi_i \leq \frac{\|A\|}{\hat{\sigma}_i^{(k)}} \sin \phi_i,$$

which, together with (4.30), proves (4.31). \square

This theorem indicates that $\hat{u}_i^{(k)}$ and $\hat{v}_i^{(k)}$ converge at least with the linear convergence factor $\frac{\gamma_{p+1}}{\gamma_i}$ but $\hat{\sigma}_i^{(k)}$ converges at least with the convergence factor $(\frac{\gamma_{p+1}}{\gamma_i})^2$. This implies that the errors of approximate singular values are roughly the squares of those of the corresponding approximate left and right singular vectors.

The bounds in Theorem 4.9 are a priori and are not available in computations. We can estimate the accuracy of an approximate singular triplet $(\hat{\sigma}_i^{(k)}, \hat{u}_i^{(k)}, \hat{v}_i^{(k)})$ in terms of its computable residual norm (2.3), as the following theorem shows.

Theorem 4.10. *For the Ritz approximations $(\hat{\sigma}_i, \hat{u}_i, \hat{v}_i)$ with the superscripts k dropped, $i = 1, 2, \dots, n_{sv}$, define*

$$\text{sep}_i = \min_{\sigma_j \neq \sigma_i} |\hat{\sigma}_i^2 - \sigma_j^2|,$$

and write the residuals $r(\hat{\sigma}_i, \hat{u}_i, \hat{v}_i) = r_i$ in (2.3). Then

$$\begin{aligned} |\hat{\sigma}_i - \sigma_i| &\leq \min \left\{ \frac{\hat{\sigma}_i \|r_i\|}{\hat{\sigma}_i + \sigma_i}, \frac{(\hat{\sigma}_i \|r_i\|)^2}{(\hat{\sigma}_i + \sigma_i) \text{sep}_i} \right\}, \\ \sin \angle(\hat{v}_i, v_i) &\leq \frac{\hat{\sigma}_i \|r_i\|}{\text{sep}_i}, \\ \sin \angle(\hat{u}_i, u_i) &\leq \frac{\|A\| \|r_i\|}{\text{sep}_i}. \end{aligned}$$

Proof. From [21, Theorem 4.5.1, Theorem 11.7.1], we obtain

$$(4.39) \quad |\hat{\sigma}_i^2 - \sigma_i^2| \leq \min \left\{ \|S \hat{v}_i - \hat{\sigma}_i^2 \hat{v}_i\|, \frac{\|S \hat{v}_i - \hat{\sigma}_i^2 \hat{v}_i\|^2}{\text{sep}_i} \right\},$$

$$(4.40) \quad \sin \angle(\hat{v}_i, v_i) \leq \frac{\|S \hat{v}_i - \hat{\sigma}_i^2 \hat{v}_i\|}{\text{sep}_i}.$$

Exploiting (4.35), we have

$$\|r_i\| = \|A^T \hat{u}_i - \hat{\sigma}_i \hat{v}_i\| = \left\| A^T \frac{A \hat{v}_i}{\hat{\sigma}_i} - \hat{\sigma}_i \hat{v}_i \right\| = \frac{\|S \hat{v}_i - \hat{\sigma}_i^2 \hat{v}_i\|}{\hat{\sigma}_i}.$$

Then combining this relation with (4.39), (4.40) and (4.37) proves the results. \square

Remark 4.11. This theorem indicates that we can determine the approximation accuracy of Ritz vectors and Ritz values by the computable residual norm. In computations, we can use the estimates $\text{sep}_i \approx \min_{\hat{\sigma}_j \neq \hat{\sigma}_i} |\hat{\sigma}_i^2 - \hat{\sigma}_j^2|$ and $\hat{\sigma}_i + \sigma_i \approx 2\hat{\sigma}_i$.

As for $\|A\|$, we have already estimated it in the beginning of section 4.1.

5. COMPUTATIONAL COST

We investigate the computational cost of Algorithm 3 and Algorithm 4. In the sequel, we count the computation of Ax or $A^T y$ as one matrix-vector product, abbreviated as MV, for given vectors x and y .

Recall that η and η_- are the replacements of $\|A\|$ and σ_{\min} . After determining

$$\frac{2}{\eta^2 - \eta_-^2} = \tilde{c}_1, \quad \frac{\eta^2 + \eta_-^2}{\eta^2 - \eta_-^2} = \tilde{c}_2,$$

the quantities in $l(x)$ defined by (4.1), we first consider the computational cost of Algorithm 3. By the three-term recurrence of Chebyshev polynomials, we have

$$\begin{aligned} T_0(l(S))z_i &= z_i, \quad T_1(l(S))z_i = l(S)z_i = \tilde{c}_1 A^T A z_i - \tilde{c}_2 z_i, \\ T_{j+1}(l(S))z_i &= 2l(S)T_j(l(S))z_i - T_{j-1}(l(S))z_i \\ &= 2\tilde{c}_1 A^T A T_j(l(S))z_i - 2\tilde{c}_2 T_j(l(S))z_i - T_{j-1}(l(S))z_i. \end{aligned}$$

We use these recursions to compute $T_j(l(S))z_i, j = 1, 2, \dots, d$ for a given z_i . The computation of $T_1(l(S))z_i$ requires two MVs and $3n$ flops, and that of $T_j(l(S))z_i$ requires two MVs and $4n$ flops for $j \geq 2$. The computation of $z_i^T T_j(l(S))z_i$ needs $2n - 1$ flops. As a result, the computation of \hat{H}_M totally requires $2Md$ MVs and approximately $6Mnd$ flops.

Now we consider the cost of one iteration in Algorithm 4.

Step 4: Similarly to the previous three-term recurrence, we have

$$\begin{aligned} T_0(l(S))\hat{V}^{(k-1)} &= \hat{V}^{(k-1)}, \quad T_1(l(S))\hat{V}^{(k-1)} = \tilde{c}_1 A^T A \hat{V}^{(k-1)} - \tilde{c}_2 \hat{V}^{(k-1)}, \\ T_{j+1}(l(S))\hat{V}^{(k-1)} &= 2\tilde{c}_1 A^T A T_j(l(S))\hat{V}^{(k-1)} - 2\tilde{c}_2 T_j(l(S))\hat{V}^{(k-1)} \\ &\quad - T_{j-1}(l(S))\hat{V}^{(k-1)}. \end{aligned}$$

The computation of $T_1(l(S))\hat{V}^{(k-1)}$ requires $2p$ MVs and $3np$ flops, and that of $T_j(l(S))\hat{V}^{(k-1)}$ requires $2p$ MVs and $4np$ flops for $j \geq 2$. So the total computational cost of $Y^{(k)}$ requires $2pd$ MVs and $4npd + np$ flops. Computing $Z^{(k)}$ requires p MVs, which means that step 4 requires $(2d + 1)p$ MVs and $4npd$ flops.

Step 5: We compute $Q_1^{(k)}$ and $Q_2^{(k)}$ by the modified Gram–Schmidt orthogonalization procedure, which requires $2(m + n)p^2$ flops [8, pp.254].

Step 6: We first compute $AQ_1^{(k)}$ and then $(Q_2^{(k)})^T (AQ_1^{(k)})$, which costs p MVs and $2mp^2$ flops.

Step 7: We compute the SVD of $\bar{A}^{(k)}$ by the Golub–Reinsch SVD algorithm, which requires about $21p^3$ flops [8, pp.493].

Step 8: This step requires $2(m + n)p^2$ flops.

Step 9: For each approximate triplet $(\hat{\sigma}, \hat{u}, \hat{v})$, because of (4.35), computing the residual norm $\|r_i\| = \|A^T \hat{u}_i - \hat{\sigma}_i \hat{v}_i\|$ requires one MV and $4n$ flops. Therefore, this step requires p MVs and $4np$ flops.

We summarize the above counts in Table 1.

Suppose that A is sparse and has $\mathcal{O}(m + n)$ nonzero entries, and assume that $p = \mathcal{O}(n_{sv})$. Then from the table we see that $p(2d + 3)$ MVs cost $\mathcal{O}(2(m + n)dn_{sv})$ flops and $4npd + 6mp^2 + 4np^2 + 21p^3 = \mathcal{O}(ndn_{sv}) + \mathcal{O}((m + n)n_{sv}^2)$. Therefore, the computation of MVs is dominant and is at least comparable to the other cost when $n \gg d > n_{sv}$. If A is not sparse and non-structured, i.e., the number of its nonzero entries is comparable to mn , then MVs cost $\mathcal{O}(2mndn_{sv})$ flops and unconditionally

Steps	MVs	Flops
4	$(2d + 1)p$	$4npd$
5		$2(m + n)p^2$
6	p	$2mp^2$
7		$21p^3$
8		$2(m + n)p^2$
9	p	$4np$
Total cost	$(2d + 3)p$	$4npd + 6mp^2 + 4np^2 + 21p^3$

TABLE 1. Computational cost of one iteration of Algorithm 4.

overwhelm the other flops. As a result, we can measure the efficiency of Algorithm 4 by the total MVs. The same applies to Algorithm 3.

6. NUMERICAL EXPERIMENTS

We now report numerical experiments and provide a detailed numerical illustration of Algorithm 4, the theoretical results and remarks. The test matrices are from The SuiteSparse Matrix Collection [4], and we list some of their basic properties and the interval $[a, b]$ of interest in Table 2. We see from the table that the conditioning of A is numerous and ranges from rank deficient to well conditioned; all the intervals $[a, b]$ are inside singular spectra, meaning that the desired singular values are not close to the largest or smallest ones and the relative interval widths differ considerably. We will also find that the numbers n_{sv} 's of the desired singular triplets differ greatly. Therefore, our SVD problems to be solved are representative in applications, implying that our test results and assertions are of generality.

Since bounding the singular spectrum of A is not our concern in this work, we will use the known results listed in the table. All the numerical experiments were performed on an Intel Core i7-9700, CPU 3.0GHz, 8GB RAM using MATLAB R2021b with the machine precision $\epsilon_{\text{mach}} = 2.22e - 16$ under the Microsoft Windows 10 64-bit system. An approximate singular triplet $(\hat{\sigma}, \hat{u}, \hat{v})$ is claimed to have converged if the relative residual norm satisfies

$$(6.1) \quad \|r(\hat{\sigma}, \hat{u}, \hat{v})\| \leq \eta \cdot \text{tol} = \eta \cdot 10^{-8},$$

where η is an estimate for $\|A\|$.

The name of A	m	n	$nnz(A)$	$\ A\ $	$\sigma_{\min}(A)$	$[a, b]$
rel8	345688	12347	821839	18.2734	0	[13, 14]
n4c6-b5	51813	20058	310878	4.58258	0	[3.2, 3.4]
GL7d12	8899	1019	37519	14.3379	$4.07e - 16$	[11, 12]
plat1919	1919	1919	32399	2.92164	$5.44e - 17$	[2.1, 2.5]
fv1	9604	9604	85264	4.51016	0.512165	[3.1, 3.15]
D6-6	120576	23740	146520	5.47723	0	[5.25, 5.3]
mk12-b3	51975	13860	207900	5.47723	$7.93e - 16$	[4.6, 5]
flower_5_4	5226	14721	43942	5.52575	0.3706071	[4.1, 4.3]

TABLE 2. Properties of test matrices, where $nnz(A)$ is the number of nonzero entries in A , and $\|A\|$, $\sigma_{\min}(A)$ are from [4].

6.1. Choices of polynomial degree and estimation of the number of desired singular values. In applications, we know nothing about the singular values of A and Δ_{\min} . A practical selection strategy for d is particularly appealing. Recall that $\theta_i = \arccos(l(\sigma_i^2))$, $i = 1, 2, \dots, n$ and $[\beta, \alpha] = [\arccos(l(b^2)), \arccos(l(a^2))]$. Without a priori information on the distribution of singular values σ_i of A , we suppose that the θ_i are uniformly distributed approximately, i.e., $\Delta_{\min} \approx \frac{\alpha-\beta}{n_{sv}}$. Then (4.17) reads as

$$d \geq \frac{\sqrt{n_{sv}n}\pi^2}{2(\alpha-\beta)} - 2.$$

As stated in Remark 4.7, this bound may be too conservative because of the conservative factor n in the pessimistic bound (4.13), it is the factor $\alpha-\beta$ in denominator that is critical and determines the accuracy of $\text{tr}(\hat{P})$ approximating n_{sv} , and the factor n behaves like $\mathcal{O}(1)$ with a modest constant in the big $\mathcal{O}(\cdot)$. On the other hand, note that $\Delta_{\min} \leq \frac{\alpha-\beta}{2}$ unconditionally. Therefore, we suggest to choose

$$(6.2) \quad d = \left\lceil \frac{C\pi^2}{\alpha-\beta} \right\rceil - 2$$

with $C \in [5, 40]$.

Theorem 4.3 indicates that d must make \hat{P} approximate P_S with some accuracy, where we have obtained a sufficient condition (4.7) on d such that (4.8) and (4.9) hold, with which the algorithm converges quite fast since $\frac{\gamma_{n_{sv}+1}}{\gamma_{n_{sv}}} < 1$ considerably. Note that (4.7) may overestimate d substantially. Therefore, we can also take d in the form of (6.2). But since d in (4.7) is smaller than that in (4.17), we suggest $C \in [2, 10]$ when using Theorem 4.3 in computations.

For our numerical justification, we need to know n_{sv} 's. To this end, we computed all the singular values of A using the standard SVD Matlab built-in code `svd`. In Table 3, we list three d 's with $C = 2, 4, 8$ and the a priori Δ_{\min} 's and the smallest integer d_0 's for which (4.7) holds. As is seen from the table, the a priori d_0 's are bigger than the corresponding d 's except for D6-6 with $C = 8$.

Matrix	Δ_{\min}	d			
		$C = 2$	$C = 4$	$C = 8$	d_0
rel8	$2.6094e-3$	120	241	484	3781
n4c6-b5	$6.6052e-3$	155	312	626	1493
GL7d12	$3.2754e-3$	83	167	335	3012
plat1919	$1.6343e-2$	42	86	174	602
fv1	$9.1211e-4$	632	1266	2533	10819
D6-6	$1.2155e-2$	289	580	1161	810
mk12-b3	$1.1668e-2$	63	127	256	844
flower_5_4	$5.5936e-4$	175	352	705	17643

TABLE 3. Δ_{\min} 's, practical d 's, and the smallest integers d_0 for which (4.7) holds.

We now confirm that \hat{H}_M with a d much smaller than that in (4.17) suffices to accurately estimate greatly varying numbers n_{sv} 's of $\sigma \in [a, b]$ for $M = 20, 30$. For each test problem, we take the polynomial degree d as (6.2) using $C = 6, 18, 40$, compute \hat{H}_{20} and \hat{H}_{30} , and list them in Table 4. Clearly, we see that, for each

Matrix	n_{sv}	M	\hat{H}_M		
			$C = 6$	$C = 18$	$C = 40$
rel8	13	20	13.5	12.4	13.4
		30	11.1	12.7	12.0
n4c6-b5	79	20	82.1	75.7	79.9
		30	83.6	79.5	76.9
GL7d12	17	20	18.4	17.3	17.1
		30	18.4	16.7	17.1
plat1919	8	20	7.0	8.0	7.7
		30	7.8	8.1	7.2
fv1	89	20	87.6	88.9	89.2
		30	89.0	86.2	91.3
D6-6	60	20	59.8	64.1	58.2
		30	60.3	61.5	59.1
mk12-b3	945	20	1256.0	953.8	943.4
		30	1268.4	958.6	937.3
flower_5_4	137	20	136.0	138.7	131.6
		30	132.7	138.6	139.3

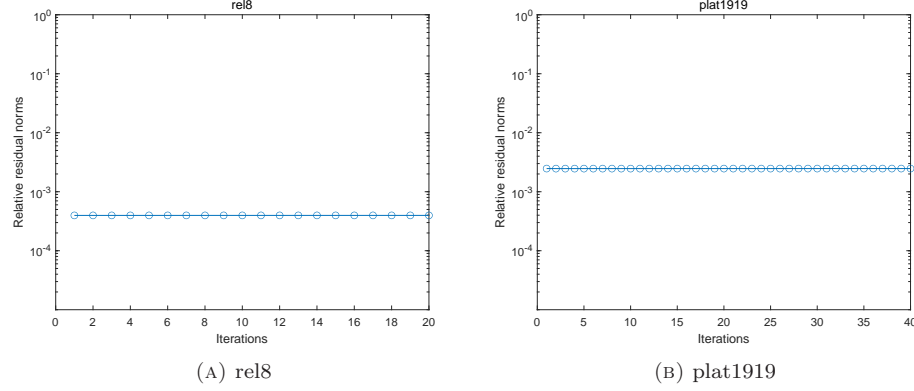
TABLE 4. The exact n_{sv} 's and theirs estimates \hat{H}_M 's.

problem, \hat{H}_M is a reliable estimate for n_{sv} , which demonstrates that the bound for $\text{tr}(\hat{P})$ in Theorem 4.5 is too conservative and $\text{tr}(\hat{P})$ estimates n_{sv} quite accurately for $M = 20, 30$. Moreover, the numerical results indicates that we always have $\lceil 1.1\hat{H}_M \rceil \geq n_{sv}$ slightly. Notice that n_{sv} 's differ greatly, from a few to over one thousand, and that both n 's and Δ_{\min} 's are quite different. The results have illustrated that our selection strategy (4.18) is reliable to ensure that the subspace dimension $p \geq n_{sv}$ in computations.

6.2. The case that the subspace dimension is smaller than the number of desired singular values. Our theoretical results and analysis imply that Algorithm 4 with $p < n_{sv}$ should not work generally since in this case we may have $\gamma_p \approx \gamma_{p+1}$. As a result, subspace iteration either converges extremely slowly or completely fails to converge if $\gamma_p = \gamma_{p+1}$. To numerically justify these predictions, we choose $d = d_0$ and $p < n_{sv}$, apply Algorithm 4 to the test matrices rel8 and plat1919, and observe its convergence behavior.

For rel8, we first take $p = n_{sv} = 13$. We observe that Algorithm 4 converges very fast and all thirteen Ritz triplets have converged when $k = 2$. But when taking $p = 12 < n_{sv}$, we find that the residual norms of all the Ritz triplets do not decrease from the first iteration to $k = 20$; in fact, the smallest relative residual norms among the twelve ones stabilize around $3.97e-4$.

We have observed similar phenomena for plat1919. For $p = n_{sv} = 8$, all the eight Ritz triplets have converged when $k = 4$. But for $p = 6 < n_{sv}$, the algorithm completely fails, and the residual norms almost stagnate from the first iteration to $k = 40$, and the smallest relative residual norms stabilize around $2.47e-3$. Figure 1 depicts the convergence processes of the smallest relative residual norms for the problems rel8 and plat1919, where it is clear that the residual norms stagnate from the first iteration onwards.

FIGURE 1. Convergence processes when $p < n_{sv}$.

These experiments have confirmed our theoretical analysis. Therefore, to make the algorithm work, one must take $p \geq n_{sv}$; unlike a flexible choice of the polynomial degree d of Chebyshev–Jackson series, the requirement $p \geq n_{sv}$ is critical.

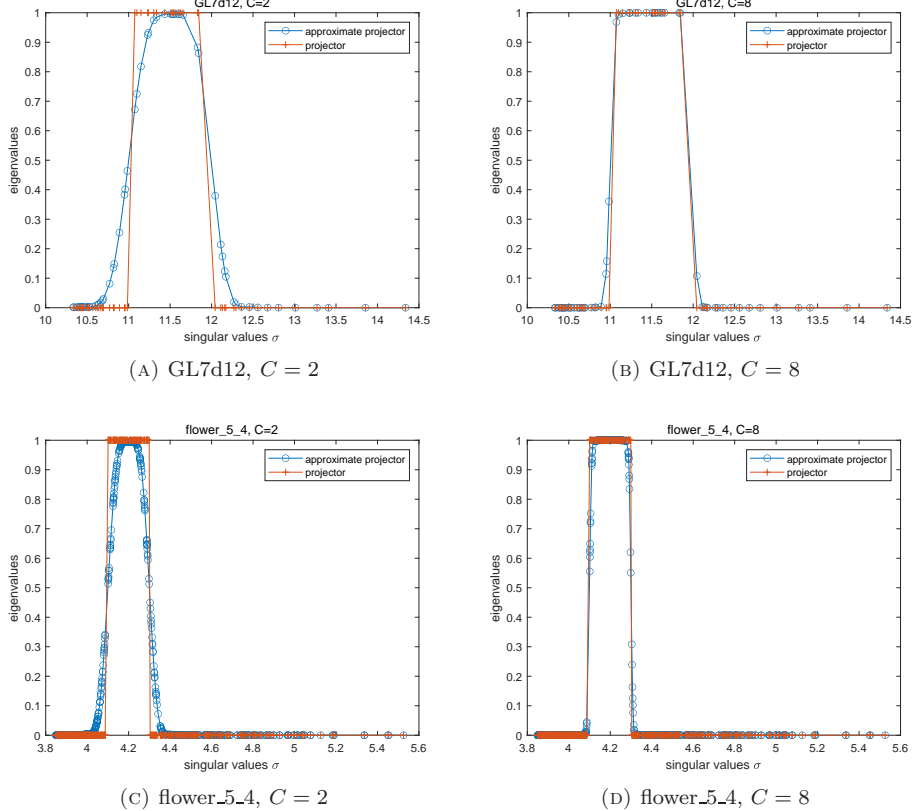
Very importantly, our analysis and numerical justification enable us to detect if $p \geq n_{sv}$ is met: for a reasonably big d , if the algorithm converges extremely slowly, then $p < n_{sv}$; we must stop the algorithm, choose a bigger $p \geq n_{sv}$ to ensure the convergence, and find the n_{sv} desired singular triplets.

6.3. Semi-definiteness of approximate spectral projector and its accuracy. We have proved that the approximate spectral projector \hat{P} is unconditionally SPSD with the eigenvalues $\gamma_i \in [0, 1]$ and established some properties of γ_i in section 4. We now confirm them numerically.

For GL7d12, from the singular values computed by the function `svd`, we have found that the right-most and left-most singular values in the interval [11, 12] are the 18-th largest one and the 34-th largest one, respectively. For flower_5_4, the right-most and left-most singular values in the interval [4.1, 4.3] are the 214-th largest one and the 350-th largest one, respectively. The ends of these two intervals are not singular values of the matrices, and the eigenvalues of P_S are thus 1 and 0, which correspond to the singular values $\sigma \in [a, b]$ and outside it, respectively. We choose $d = \left\lceil \frac{C\pi^2}{\alpha-\beta} \right\rceil - 2$ using $C = 2$ and 8, compute the eigenvalues γ_i , $i = 1, 2, \dots, n$ of \hat{P} , and depict the points γ_i corresponding to $\sigma_i \in [a, b]$ and some neighbors outside in Figure 2. We record $\|P_S - \hat{P}\|$, $\gamma_{n_{sv}}$ and $\gamma_{n_{sv}+1}$, the largest γ_1 and smallest γ_n , and γ_{p+1} for $p = \lceil \mu \hat{H}_M \rceil$ by taking $\mu = 1.1, 1.2, 1.3, 1.4, 1.5$, respectively, and list them in Table 5.

Matrix	d	$\ P_S - \hat{P}\ $	$\gamma_{n_{sv}}$	$\gamma_{n_{sv}+1}$	γ_1	γ_n	γ_{p+1}				
							$\mu = 1.1$	$\mu = 1.2$	$\mu = 1.3$	$\mu = 1.4$	$\mu = 1.5$
GL7d12	$C = 2$	0.4641	0.6722	0.4641	0.9953	$7.35e-7$	$3.83e-1$	$2.55e-1$	$1.74e-1$	$1.48e-1$	$1.24e-1$
	$C = 8$	0.3602	0.9694	0.3602	0.9999	$1.19e-8$	$1.15e-2$	$3.23e-3$	$1.98e-3$	$1.21e-3$	$6.82e-4$
flower_5_4	$C = 2$	0.4875	0.5125	0.4501	0.9953	$4.67e-8$	$2.98e-1$	$1.96e-1$	$1.35e-1$	$5.49e-2$	$3.06e-2$
	$C = 8$	0.4491	0.5509	0.3084	0.9999	$7.54e-10$	$1.20e-2$	$2.40e-3$	$8.41e-4$	$3.18e-4$	$1.95e-4$

TABLE 5. $\|P_S - \hat{P}\|$ and some eigenvalues of \hat{P} .

FIGURE 2. The eigenvalues of \hat{P} .

Several comments are in order on the figure and the table. First, for each matrix, the two \hat{P} 's generated by two C 's are all SPSD since all the $\gamma_n > 0$. Second, the eigenvalues of each \hat{P} are indeed in $[0, 1]$ since all the $\gamma_1 < 1$. Third, γ_i decay fast outside the given interval, and their sizes indeed differ greatly as i increases, which justifies Remark 4.7 and confirms that bound (4.16) and thus bound (4.13) are severely conservative. Fourth, for each C , the slowest convergence factor $\frac{\gamma_{p+1}}{\gamma_{n_{sv}}} < \frac{\gamma_{n_{sv}+1}}{\gamma_{n_{sv}}}$ considerably as μ , i.e., p , increases; the bigger C is, the closer to one γ_1 is, the smaller are $\gamma_{n_{sv}+1}$ and γ_{p+1} . This shows that the subspace dimension $p > n_{sv}$ slightly is necessary and may speed up the convergence of the FEAST SVDsolver considerably.

6.4. General numerical results and a practical selection strategy for subspace dimension. The slowest convergence rate $\frac{\gamma_{p+1}}{\gamma_{n_{sv}}}$ of Algorithm 4 is not affected by $p \geq n_{sv}$ significantly when $\gamma_{p+1} \approx \gamma_{n_{sv}+1}$, which may be true as (4.12) shows that γ_j , $j = n_{sv}+1, \dots, n$ are small for d big and monotonically decrease to zero as d increases. Definitely, for d large enough, ϵ in (4.12) will be indeed small, so that the algorithm converges very fast; in this case, it is best to take $p \approx n_{sv}$, a bigger p not only does not reduce iterations needed but also costs more MVs and other

flops correspondingly in Table 1. However, given a not large d , it is possible that $\frac{\gamma_{n_{sv}+1}}{\gamma_{p+1}} > 1$ considerably since they satisfy (4.12) for some not small ϵ . We have numerically demonstrated these findings in the last subsection. Therefore, the size of p may have a substantial effect on the convergence rate. To be safe, it is better to take $p > n_{sv}$ more or less.

For each test matrix, we take the series degree d as (6.2) using $C = 2, 4, 8$ and $d = d_0$ in Table 3, and select the subspace dimensions $p = n_{sv}, \lceil 1.1\hat{H}_M \rceil, \lceil 1.2\hat{H}_M \rceil$ and $\lceil 1.5\hat{H}_M \rceil$, where \hat{H}_M is the closest one to n_{sv} selected from Table 4. We then use Algorithm 4 to solve the concerning SVD problems, record the total MVs and numbers of iterations required for convergence, and list them in Table 6, where $\text{MVs}(k)$ denotes the numbers of MVs and k in the braces is the number of iterations that the norms of all the approximate singular triplets satisfy (6.1). For each problem and the same p , we used the same orthonormal initial $\hat{V}^{(0)}$ generated by the QR factorization of p random vectors in normal distribution.

Combining Table 3 with Table 6, we make some comments on the results obtained. We first investigate the case that $p \geq n_{sv}$ is fixed but d changes. First, for each given p , the algorithm converged quite fast for the three d 's and d_0 , and it used fewer iterations as the series degree d increases. Second, for all the test problems but D6-6, the algorithm with d_0 converged very fast and often used considerably fewer iterations than it did with the other three d 's, but it consumed more and, sometimes, substantially more MVs than the latter did and was thus (much) less efficient. Third, for D6-6, the algorithm converged very fast and used very few iterations to converge. Fourth, for a given p , the algorithm with the three d 's consumed comparable MVs for each problem, indicating that the overall efficiency is insensitive to d and a flexible choice of d is allowed.

Next we look at the case that d is fixed but p changes. First, for all the test problems but D6-6, the algorithm used fewer iterations for a bigger p , as expected. Second, for D6-6, the algorithm converged very fast and used only $2 \sim 4$ iterations for three p 's; our algorithm solved this problem very easily. Third, the algorithm with $p = \lceil 1.1\hat{H}_M \rceil, \lceil 1.2\hat{H}_M \rceil$ and $\lceil 1.5\hat{H}_M \rceil$ generally converged considerably faster than the algorithm with $p = n_{sv}$, though $p = \lceil 1.1\hat{H}_M \rceil > n_{sv}$ only slightly. These support the suggestion that we should choose $p > n_{sv}$ rather than $p = n_{sv}$. Fourth, the algorithm with $p = \lceil 1.5\hat{H}_M \rceil$ converged fastest, but its overall efficiency depends critically on the required iterations. When the algorithm used very substantially fewer iterations than it did with $p = \lceil 1.1\hat{H}_M \rceil, \lceil 1.2\hat{H}_M \rceil$, it saved MVs; but the latter often used the same or comparable iterations as the former, especially when d is reasonably large. Consequently, the algorithm with $p = \lceil 1.5\hat{H}_M \rceil$ consumed more MVs. Therefore, for a general purpose, it is preferable to use $p = \lceil 1.1\hat{H}_M \rceil$ or $\lceil 1.2\hat{H}_M \rceil$.

Finally, we illustrate the convergence processes of Algorithm 4 using two examples and highlight some features of it.

For *rel8* with $n_{sv} = 13$, take $d = \lceil \frac{4\pi^2}{\alpha-\beta} \rceil - 2 = 241$ and $p = 16$. We found that all the desired approximate singular triplets converged at $k = 8$ and the most slowly converged singular value is 13.984665903216340. We plot the residuals norms of the corresponding Ritz approximations, errors of the Ritz values and error bounds in Theorem 4.10 in Figure 3a.

Matrix	p	MVs (k)			
		$C = 2$	$C = 4$	$C = 8$	d_0
rel8	13	$1.67e + 5$ (53)	$1.58e + 5$ (25)	$1.39e + 5$ (11)	$1.97e + 5$ (2)
	14	$1.39e + 5$ (41)	$1.29e + 5$ (19)	$1.09e + 5$ (8)	$2.12e + 5$ (2)
	16	$7.39e + 4$ (19)	$6.21e + 4$ (8)	$4.66e + 4$ (3)	$2.42e + 5$ (2)
	20	$5.83e + 4$ (12)	$3.88e + 4$ (4)	$5.83e + 4$ (3)	$3.03e + 5$ (2)
n4c6-b5	79	$6.43e + 5$ (26)	$7.43e + 5$ (15)	$7.93e + 5$ (8)	$9.45e + 5$ (4)
	88	$6.34e + 5$ (23)	$7.17e + 5$ (13)	$7.73e + 5$ (7)	$7.89e + 5$ (3)
	96	$5.41e + 5$ (18)	$6.02e + 5$ (10)	$4.82e + 5$ (4)	$8.61e + 5$ (3)
	120	$6.01e + 5$ (16)	$6.02e + 5$ (8)	$6.02e + 5$ (4)	$1.08e + 6$ (3)
GL7d12	17	$1.21e + 5$ (42)	$1.43e + 5$ (25)	$1.94e + 5$ (17)	$3.07e + 5$ (3)
	19	$8.35e + 4$ (26)	$9.60e + 4$ (15)	$1.02e + 5$ (8)	$3.44e + 5$ (3)
	21	$7.10e + 4$ (20)	$6.37e + 4$ (9)	$5.65e + 4$ (4)	$2.53e + 5$ (2)
	26	$4.40e + 4$ (10)	$4.38e + 4$ (5)	$5.25e + 4$ (3)	$3.13e + 5$ (2)
plat1919	8	$2.02e + 4$ (29)	$2.24e + 4$ (16)	$3.09e + 4$ (11)	$2.90e + 4$ (3)
	9	$2.19e + 4$ (28)	$2.52e + 4$ (16)	$3.16e + 4$ (10)	$3.26e + 4$ (3)
	10	$6.96e + 3$ (8)	$7.00e + 3$ (4)	$1.05e + 4$ (3)	$2.41e + 4$ (2)
	12	$8.35e + 3$ (8)	$8.40e + 3$ (4)	$1.26e + 4$ (3)	$2.90e + 4$ (2)
fv1	89	$4.96e + 6$ (44)	$5.64e + 6$ (25)	$5.41e + 6$ (12)	$5.78e + 6$ (3)
	98	$2.98e + 6$ (24)	$2.73e + 6$ (11)	$1.99e + 6$ (4)	$4.24e + 6$ (2)
	107	$1.22e + 6$ (9)	$1.08e + 6$ (4)	$1.63e + 6$ (3)	$4.63e + 6$ (2)
	134	$8.49e + 5$ (5)	$1.02e + 6$ (3)	$2.04e + 6$ (3)	$5.80e + 6$ (2)
D6-6	60	$6.97e + 4$ (2)	$1.40e + 5$ (2)	$2.79e + 5$ (2)	$1.94e + 5$ (2)
	66	$7.67e + 4$ (2)	$1.54e + 5$ (2)	$3.07e + 5$ (2)	$2.14e + 5$ (2)
	72	$8.37e + 4$ (2)	$1.67e + 5$ (2)	$3.35e + 5$ (2)	$2.34e + 5$ (2)
	90	$1.04e + 5$ (2)	$2.09e + 5$ (2)	$4.19e + 5$ (2)	$2.92e + 5$ (2)
mk12-b3	945	$3.41e + 6$ (28)	$4.61e + 6$ (19)	$6.32e + 6$ (13)	$7.99e + 6$ (5)
	1038	$2.95e + 6$ (22)	$4.27e + 6$ (16)	$5.35e + 6$ (10)	$7.02e + 6$ (4)
	1133	$3.22e + 6$ (22)	$4.66e + 6$ (16)	$5.83e + 6$ (10)	$5.75e + 6$ (3)
	1416	$3.84e + 6$ (21)	$5.46e + 6$ (15)	$7.29e + 6$ (10)	$7.18e + 6$ (3)
flower_5_4	137	$6.19e + 6$ (128)	$6.01e + 6$ (62)	$5.61e + 6$ (29)	$9.67e + 6$ (2)
	150	$1.69e + 6$ (32)	$1.59e + 6$ (15)	$1.27e + 6$ (6)	$1.06e + 7$ (2)
	164	$1.10e + 6$ (19)	$8.12e + 5$ (7)	$9.27e + 5$ (4)	$1.16e + 7$ (2)
	204	$5.04e + 5$ (7)	$5.77e + 5$ (4)	$8.65e + 5$ (3)	$1.44e + 7$ (2)

TABLE 6. We choose different d and p and record total MVs and numbers of iterations required for convergence, where total MVs are represented by scientific notation and retain 3 significant digits.

For GL7d12 with $n_{sv} = 17$, we choose $d = \lceil \frac{4\pi^2}{\alpha-\beta} \rceil - 2 = 167$ and $p = 21$. All the desired approximate singular triplets converged at $k = 8$, and the most slowly converged singular value is 11.074228368664937. We draw the convergence process in Figure 3b in a way similar to Figure 3a.

As is clear from the figure, for each problem, the residual norms and errors of Ritz values decrease linearly but at different convergence rates, and the error of Ritz values is roughly squares of the residual norm at the same iteration. This means that the accuracy of Ritz value is about the square of the residual norm, confirming the a priori bound in Theorem 4.9 and the a posteriori bound in Theorem 4.10. In addition, we observe from the figure that the error bounds for Ritz values predict

the decreasing trend of the true errors accurately and they are only about one or two orders larger than the true errors.

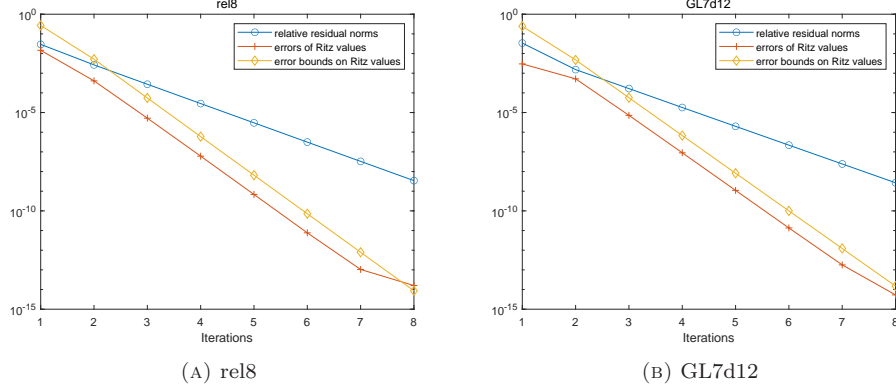


FIGURE 3. Convergence processes of residual norms, errors of Ritz values and their bounds.

7. CONCLUSIONS

We have considered the problem of approximating the step function $h(x)$ in (3.1) by the Chebyshev–Jackson series expansion and derived quantitative pointwise error bounds. Making use of these results, we have established quantitative accuracy estimates for the approximate spectral projector constructed by the series as an approximation to the spectral projector P_S of A associated with all the singular values $\sigma \in [a, b]$. Based on these results, we have developed the FEAST SVDSolver for the computation of the singular triplets with $\sigma \in [a, b]$. We have analyzed the convergence of the algorithm and proved how the subspaces constructed converge to the desired right singular subspace and how each of the Ritz approximations converges as iterations proceed. Remarkably, the convergence of our FEAST SVDSolver is always guaranteed since we can always construct an approximate spectral projector with necessary accuracy. In the meantime, we have discussed how to select the subspace dimension p and the series degree d in computations, and proposed robust and general-purpose selection strategies for them.

Unlike a contour integral-based FEAST eigensolver, where P_S is expressed as a contour integral and is approximated by a numerical quadrature, which needs to solve a sequence of large shifted linear systems whose number is the number of nodes times the subspace dimension at each iteration. In order to ensure that the FEAST solver converges linearly, approximate solutions of the shifted linear systems must have increasing accuracy as outer iterations proceeds [7, 31], causing that the method may be very costly. Even worse, the accuracy requirement may not be ensured when a shifted linear system is ill conditioned. This is a potential difficulty but has received little attention: if at least one shifted linear system is ill conditioned, which occurs when a node is close to an eigenvalue, it is well known that an approximate solution may have very poor and even no accuracy at all even if its residual norm is already very small in finite precision arithmetic. As is pointed out

in [19], such a case occurs more possibly for the non-Hermitian matrix eigenvalue problem. It could also occur in the Hermitian case, and a possible remedy is to take nodes away from the real axis. In contrast, we can always construct an approximate spectral projector with *required* accuracy, provided that the series degree d is suitably chosen. Moreover, the construction of an approximate spectral projector by the Chebyshev–Jackson series expansion involves only matrix-matrix products and can thus be implemented very efficiently in parallel computing environments.

Another considerable difference is that the approximate spectral projector constructed by the Chebyshev–Jackson series is unconditionally SPSD but that constructed by numerical quadratures is generally not even though all the shifted linear systems are solved accurately. As we have seen, SPSD is very important and enables us to reliably estimate the number n_{sv} of desired singular triplets and propose a robust selection strategy for the subspace dimension $p \geq n_{sv}$.

We have numerically tested our FEAST SVDsolver on a number of problems in several aspects and shown that it is robust, effective and efficient.

Our theoretical analysis and results can be directly applied or trivially adapted to the real symmetric or complex Hermitian matrix eigenvalue problem, where the eigenpairs with the eigenvalues in a given real interval are of interest. The adaptation of the FEAST SVDsolver to this kind of eigenvalue problem is straightforward, where we only need to replace the Rayleigh–Ritz projection for the SVD problem by the one for the eigenvalue problem and the practical selection strategies proposed for p and d still work.

REFERENCES

- [1] H. Avron and S. Toledo, *Randomized algorithms for estimating the trace of an implicit symmetric positive semi-definite matrix*, J. ACM **58** (2011), no. 2, Art. 8, 17. MR2786589
- [2] C. Bekas, E. Kokiopoulou, and Y. Saad, *An estimator for the diagonal of a matrix*, Appl. Numer. Math. **57** (2007), no. 11–12, 1214–1229. MR2355413
- [3] A. Cortinovis and D. Kressner, *On randomized trace estimates for indefinite matrices with an application to determinants*, Found. Comput. Math. (2021).
- [4] T. A. Davis and Y. Hu, *The University of Florida sparse matrix collection*, ACM Trans. Math. Software **38** (2011), no. 1, Art. 1, 25. MR2865011
- [5] E. Di Napoli, E. Polizzi, and Y. Saad, *Efficient estimation of eigenvalue counts in an interval*, Numer. Linear Algebra Appl. **23** (2016), no. 4, 674–692. MR3522849
- [6] Y. Futamura and T. Sakurai, *z-Pares: Parallel Eigenvalue Solver*, 2014.
- [7] B. Gavin and E. Polizzi, *Krylov eigenvalue strategy using the FEAST algorithm with inexact system solves*, Numer. Linear Algebra Appl. **25** (2018), no. 5, e2188, 20. MR3859165
- [8] G. H. Golub and C. F. Van Loan, *Matrix Computations*, Fourth Edition, Johns Hopkins Studies in the Mathematical Sciences, Johns Hopkins University Press, Baltimore, MD, 2013. MR3024913
- [9] S. Güttel, E. Polizzi, P. T. P. Tang, and G. Viaud, *Zolotarev quadrature rules and load balancing for the FEAST eigensolver*, SIAM J. Sci. Comput. **37** (2015), no. 4, A2100–A2122. MR3384838
- [10] M. F. Hutchinson, *A stochastic estimator of the trace of the influence matrix for Laplacian smoothing splines*, Comm. Statist. Simulation Comput. **18** (1989), no. 3, 1059–1076. MR1031840
- [11] T. Iitaka and T. Ebisuzaki, *Random phase vector for calculating the trace of a large matrix*, Phys. Rev. E **69** (2004), no. 5, e057701, 4.
- [12] T. Ikegami and T. Sakurai, *Contour integral eigensolver for non-Hermitian systems: a Rayleigh–Ritz-type approach*, Taiwanese J. Math. **14** (2010), no. 3, 825–837. MR2667719
- [13] T. Ikegami, T. Sakurai, and U. Nagashima, *A filter diagonalization for generalized eigenvalue problems based on the Sakurai–Sugiura projection method*, J. Comput. Appl. Math. **233** (2010), no. 8, 1927–1936. MR2564028

- [14] A. Imakura, L. Du, and T. Sakurai, *A block Arnoldi-type contour integral spectral projection method for solving generalized eigenvalue problems*, Appl. Math. Lett. **32** (2014), 22–27. MR3182841
- [15] ———, *Relationships among contour integral-based methods for solving generalized eigenvalue problems*, Jpn. J. Ind. Appl. Math. **33** (2016), no. 3, 721–750. MR3579284
- [16] L. O. Jay, H. Kim, Y. Saad, and J. R. Chelikowsky, *Electronic structure calculations for plane-wave codes without diagonalization*, Comput. Phys. Commun. **118** (1999), no. 1, 21–30.
- [17] Z. Jia and D. Niu, *An implicitly restarted refined bidiagonalization Lanczos method for computing a partial singular value decomposition*, SIAM J. Matrix Anal. Appl. **25** (2003), no. 1, 246–265. MR2002911
- [18] ———, *A refined harmonic Lanczos bidiagonalization method and an implicitly restarted algorithm for computing the smallest singular triplets of large matrices*, SIAM J. Sci. Comput. **32** (2010), no. 2, 714–744. MR2609338
- [19] J. Kestyn, E. Polizzi, and P. T. P. Tang, *FEAST eigensolver for non-Hermitian problems*, SIAM J. Sci. Comput. **38** (2016), no. 5, S772–S799. MR3565586
- [20] J. C. Mason and D. C. Handscomb, *Chebyshev polynomials*, Chapman & Hall/CRC, Boca Raton, FL, 2003. MR1937591
- [21] B. N. Parlett, *The Symmetric Eigenvalue Problem*, Classics in Applied Mathematics, vol. 20, Society for Industrial and Applied Mathematics (SIAM), Philadelphia, PA, 1998. Corrected reprint of the 1980 original. MR1490034
- [22] E. Polizzi, *Density-matrix-based algorithm for solving eigenvalue problems*, Phys. Rev. B **79** (2009), no. 11, e115112, 6.
- [23] ———, *FEAST eigenvalue solver v4.0 user guide*, 2020.
- [24] T. J. Rivlin, *An introduction to the approximation of functions*, Dover Books on Advanced Mathematics, Dover Publications, Inc., New York, 1981. Corrected reprint of the 1969 original. MR634509
- [25] F. Roosta-Khorasani and U. Ascher, *Improved bounds on sample size for implicit matrix trace estimators*, Found. Comput. Math. **15** (2015), no. 5, 1187–1212. MR3394708
- [26] Y. Saad, *Iterative methods for sparse linear systems*, Second, Society for Industrial and Applied Mathematics, Philadelphia, PA, 2003. MR1990645
- [27] ———, *Numerical methods for large eigenvalue problems*, Classics in Applied Mathematics, vol. 66, Society for Industrial and Applied Mathematics (SIAM), Philadelphia, PA, 2011. Revised edition of the 1992 original [1177405]. MR3396212
- [28] T. Sakurai and H. Sugiura, *A projection method for generalized eigenvalue problems using numerical integration*, Proceedings of the 6th Japan-China Joint Seminar on Numerical Mathematics (Tsukuba, 2002), 2003, pp. 119–128. MR2022322
- [29] T. Sakurai and H. Tadano, *CIRR: a Rayleigh-Ritz type method with contour integral for generalized eigenvalue problems*, Hokkaido Math. J. **36** (2007), no. 4, 745–757. MR2378289
- [30] G. W. Stewart, *Matrix Algorithms. Vol. II*, Society for Industrial and Applied Mathematics (SIAM), Philadelphia, PA, 2001. Eigensystems. MR1853468
- [31] P. T. P. Tang and E. Polizzi, *FEAST as a subspace iteration eigensolver accelerated by approximate spectral projection*, SIAM J. Matrix Anal. Appl. **35** (2014), no. 2, 354–390. MR3188390
- [32] M. N. Wong, F. J. Hickernell, and K. I. Liu, *Computing the trace of a function of a sparse matrix via Hadamard-like sampling*, Department of Mathematics, Hong Kong Baptist University, 2004.

CORRESPONDING AUTHOR. DEPARTMENT OF MATHEMATICAL SCIENCES, TSINGHUA UNIVERSITY, 100084 BEIJING, CHINA

Email address: `jiazx@tsinghua.edu.cn`

DEPARTMENT OF MATHEMATICAL SCIENCES, TSINGHUA UNIVERSITY, 100084 BEIJING, CHINA
Email address: `zkl18@mails.tsinghua.edu.cn`